

AB INITIO CALCULATION OF OPTICAL ABSORPTION AND OPTICAL GAP OF SILICON NANOCRYSTALLITES

A thesis submitted to the School of Graduate Studies
Addis Ababa University



In partial Fulfilment of the Requirements for the
Degree of Master of Science in Physics

By
Derese Gugsu

Addis Ababa, Ethiopia

July 2007

ADDIS ABABA UNIVERSITY
FACULTY OF SCIENCE
DEPARTMENT OF PHYSICS

The undersigned hereby certify that they have read and recommended to the Faculty of Science School of Graduate Studies for acceptance a thesis entitled “**Ab Initio calculation of optical absorption and optical gap of silicon nanocrystallites**” by **Derese Gugsa** in partial fulfillment of the requirements for the degree of **Master of Science in Physics**.

Name

Signature

Dr. S.K Ghoshal, Advisor

Professor P. Singh, Examiner

Dr. Tesgera Bedassa , Examiner

TO MY PARENTS

Acknowledgements

First of all, I would like to express my sincere thanks to my supervisor, Dr. S.K. Ghoshal for his kind guidance and instructions throughout the period of the thesis. I also would like to express my sincere gratitude to Mekelle University to give me opportunity to study at Addis Ababa University. Finally, I appreciate the cooperation of all of my colleagues at Addis Ababa University especially and helpful attitude toward me. Once again, I would like to thank Dr. S.K Ghoshal, my supervisor, for his many suggestions and constant support during this research.

Finally, I am grateful to my parents for their patience and *love*. Without them this work would never have come into existence.

Addis Ababa, Ethiopia

Derese Gugsa

Abstract

The electronic and optical properties of hydrogenated silicon nanocrystals have been investigated both in the ground- and in an excited-state configuration, through different ab-initio techniques. The presence of an electron-hole pair leads to a strong interplay between the structural and optical properties of the system. The aim of this work was to investigate the optical properties of hydrogenated Si nanoclusters (H-Si-nc) that has recent experimental interest for photonic applications. The optical absorption spectra of small Si_nH_m nanoclusters are computed using a linear response theory within the time-dependent local density approximation (TDLDA). The TDLDA formalism allows the electronic screening and correlation effects, which determine exciton binding energies, to be naturally incorporated within an ab initio framework. We examined that the calculated excitation energies and optical absorption gaps to be in good agreement with experiment.

Table of Contents

Table of Contents	vi
List of Tables	vii
List of Figures	viii
Introduction	1
1 Theoretical Methods	5
1.1 Density Functional Theory	6
1.1.1 Local Density Approximation	9
1.1.2 Pseudopotential Approximation	10
1.2 Time-dependent Density Functional Theory	13
2 Time Dependent Density Functional Based Linear Response Theory	17
2.1 Time Dependent Response Theory	17
2.1.1 Derivation of Generalized Susceptibility	18
2.2 Linear Response of the Density Matrix	21
3 Results for Excitation Energies and Optical Gap	26
3.1 Calculation of Excitation Energies and Oscillator Strength	26
3.2 Approximation of the Exchange-Correlation Kernel	30
3.3 Calculation of Optical Gap	34
3.4 Computational Methods	37
4 Result and Discussion	40
5 Conclusion	48
Bibliography	50

List of Tables

3.1	Fitting parameters in the interpolation formula for the correlation energy given by Eq.(3.30). The data is taken from Ref. [8].	32
3.2	Expansion coefficients C_n $n = 0, \dots, \pm N$, for higher-order finite-difference expressions of the second derivative [12].	38
4.1	Excitation and ionization energies of Si_nH_m clusters. Experimental excitation energies are adapted from Ref. [10]. All values are in eV. . .	42

List of Figures

1.1	Schematic representation of a pseudopotential (left, dark curve) and a pseudo-wavefunction (right, dark curve) along with the all-electron potential (with the $1/r$ tail) and wavefunction (light curves). Notice that the all-electron and pseudo-functions are identical beyond the radial cutoff r_c and the pseudo-functions are smooth outside the core region.	12
3.1	Uniform grid illustrating a typical configuration for examining the electronic structure of a localized system. The gray sphere represents the domain where the wavefunctions are allowed to be non-zero. The light spheres within the domain are atoms.	38
4.1	Optimized Structure of Si_nH_m clusters.	41
4.2	Photoabsorption versus photon energy for Si_nH_m clusters.	43
4.3	Excitation energy versus cluster diameter.	44
4.4	Oscillator strength versus Si_nH_m cluster diameter	45
4.5	Oscillator strength versus number of silicon atom in the cluster.	45
4.6	Variation of optical absorption gaps as a function of cluster diameter.	46
4.7	LUMO-HOMO band gap versus the effective sizes from Wang and Zunger (triangles), multi band effective mass result (stars), the result of the method of Rama Krishna and Friesner (square boxes) and our result without hydrogen (plus) and with hydrogen (solid circles) [11].	47

Introduction

Atomic clusters are aggregates containing from few to a few thousand atoms. Due to their small nanometric or sub-nanometric size, many properties of the clusters are different from those of the corresponding macroscopic material. Those differences arise from the fact that a substantial fraction of atoms form the cluster surface, while this fraction becomes negligible in the case of a macroscopic (bulk) piece of material. Many of the properties of clusters can also be understood as arising from the small volume of the potential well that confines the electrons. In this case the electrons fill discrete levels. An interesting question which still lacks a convincing answer is the following: how many atoms are required for a cluster to show the properties of the bulk material? But, even more important is the fact that the variation of a given property like the cluster geometry, or the values of the ionization potential, is often not smooth as the number of atoms in the cluster increases one by one. This possibility of tuning the value of a given magnitude by changing the number of atoms in the cluster opens up enormous possibilities for the technological applications of these interesting nanostructures. It becomes necessary to characterize the electronic, structural and chemical properties of clusters, and the optical, photo-electron and time-resolved spectroscopies help in this task, allowing the study of static and dynamic electron-electron correlations. The electronic levels are quantized in atomic clusters

and nanostructures, reflecting the behavior of electrons in a potential well of finite size. The optical spectrum provides information on the electronic structure. It is sensitive to the size and the geometrical structure of the cluster. This is an important feature, since the knowledge of the geometrical structure is required for understanding many cluster properties. The ab initio methods captures powerful information about structural and other properties of nanostructures.

In silicon nanocrystals the electronic states as compared to bulk silicon are dramatically influenced by the enhanced role of states- and defects- at the surface. The effect of quantum confinement is a rearrangement of the density of electronic states in energy as direct consequence of volume shrinking in one, two or three dimensions, which can be obtained, respectively, in quantum wells, wires and dots. On the other hand, the arrangement of atomic bonds at the surface also strongly affects the energy distribution of electronic states, since in silicon nanocrystals the silicon atoms are either at the surface or few lattice sites away. The quantum confinement and suitable arrangement of interfacial atomic bonds can provide in silicon nanocrystals radiative recombination efficiencies that are orders of magnitude larger than in bulk silicon, which accounts for its great technological applications in the field of photonics.

Understanding the spectroscopic properties of clusters means understanding their response to time-dependent external fields. We are interested in the response to an external field that is not strong, and in such a case it is enough to consider the linear response to the external field. We are confronted with many-electron systems, for which the straightforward solution of the *Schrödinger* equation is computationally unattainable. The methods based on the many-body wavefunction, such as the traditional quantum chemistry approaches, or Quantum-Monte Carlo techniques, are

possible alternatives, but their computing requirements grow rapidly with the size of the system. This problem is already severe when dealing with ground-state properties (total energy calculations), or when attempting to do lowest order perturbation theory. In the last decades, it has been shown how the problem of the ground and excited state properties of clusters can be conveniently attacked, for many purposes, with the help of density-functional theory (DFT) [1]. In particular, many excited state properties (e.g., the spectrum of optical excitations) can be calculated by the so called time-dependent density-functional theory (TDDFT) [2].

In this thesis we propose a different approach to the calculation of excitation energies which is based on a time-dependent local density approximation. The TDLDA technique can be viewed as a natural extension of the ground state density-functional LDA formalism, designed to include the proper representation of excited states. TDLDA excitation energies of a many-electron system are usually computed from conventional, time-independent Kohn-Sham transition energies and wavefunctions. Compared to other theoretical methods for excited states, the TDLDA technique requires considerably less computational effort. Despite its relative simplicity, the TDLDA method incorporates screening and relevant correlation effects for electronic excitations. In this sense, TDLDA represents a fully ab initio formalism for excited states.

To extract excitation energies from TDLDA we exploit the fact that the frequency dependent linear response of a finite interacting system has discrete poles at the excitation energies $\omega_I = E_I - E_0$ of the unperturbed system. The idea is to calculate the shift of the Kohn-Sham orbital energy differences $\omega_{jk} = \epsilon_j - \epsilon_k$ (which are the poles of the Kohn-Sham response function) towards the true excitation energies ω_I .

To this end we first derive a formally exact representation of the linear density response $\rho(r, \omega)$ in terms of the Kohn-Sham response function and a frequency dependent exchange-correlation Kernel, which will be used to calculate the shift of the poles. To determine the optical gap of hydrogenated nano-silicon we have calculated the quasi-particle gap and exciton Coulomb energy from the knowledge of time-independent Kohn-Sham orbitals first then the optical gap is simply the difference between the quasi-particle gap and the exciton Coulomb energy. Finally, our results are compared with experimental data, showing that our calculations are in conformity with it. Lastly, we have concluded the result of our theoretical investigation.

Chapter 1

Theoretical Methods

In this chapter we revise the theoretical foundations of the methods and calculations that are employed in the thesis: density functional theory, both in its original formulation (DFT) and in its time-dependent version (TDDFT). We will only make a brief exposition of the basic principles, with no attempt to discuss mathematical subtleties. Since the theory itself is not the objective of the thesis, rather how the essence of it can be exploited for the nanostructure. Notwithstanding this, it is necessary to establish the origin and justification of the equations that are later on used in all the applications. The first two sections of this chapter revise respectively DFT and TDDFT: we enunciate the fundamental theorems that constitute the basis of the theories.

1.1 Density Functional Theory

Theoretically, the properties of solid can be obtained by solving the eigenstates of total Hamiltonian of the system. In the atomic unit system, non-relativistic Hamiltonian of the system is given by

$$H = -\frac{1}{2} \sum_i \nabla_i^2 + \frac{1}{2} \sum_{i \neq j} \frac{e^2}{|\mathbf{r}_i - \mathbf{r}_j|} + \sum_i V_{ion}(\mathbf{r}_i) + E_{ion}(\{\mathbf{R}_n\}), \quad (1.1)$$

where i - j - summations take over all electron positions, \mathbf{R}_n is n^{th} -atom position. $V_{ion}(\mathbf{r}_i)$ is atom potential at \mathbf{r}_i , and $E_{ion}(\{\mathbf{R}_n\})$ is the ion-ion direct interaction.

Most of the properties of the system being in interest such as the total energy of the ground state, electron density and electrostatic potential, etc., can be obtained by solving *Schrödinger* equation:

$$H\Psi_0(\{\mathbf{r}_i\}) = E_0\Psi_0(\{\mathbf{r}_i\}). \quad (1.2)$$

One of attempts of non-empirical method to obtain the properties of solid is to solve the equation of the many-electron Hamiltonian Eq.(1.1) directly. In practice, equation (1.2) is often rewritten through a Slater determinant which is composed of a lot of single-electron wavefunctions. This is the so-called Hartree-Fock approximation, where only the exchange effect is considered. In many problems, it is known that the exchange term only is not good. Further developments in order to include the correlation effect into account, many methods, such as the configuration interaction by expanding on many Slater determinants and the quantum Monte Carlo method, etc., have been devised.

These approaches are all based upon the wavefunctions and express the electronic states of solid through the set of wavefunctions. In the configuration interaction

method, the combination of wavefunctions is very complicated, resulting in severely the limitation of the size of problems.

Meanwhile, for the many-electron problems, another and very different approach called the density functional theory has been proposed. In this approach, the electron density is the quantity, from which the theory is developed. To solve one-electron equations which are derived from the density functional theory is much easier than solving Eq. (1.2). The correlation effect is taken into account, and the size of the system which can be handled is far larger. Since 1980, this method has established a position as one of the main methods of calculating the properties of solid and molecules from the first principles (called *ab initio*).

The work by Hohenberg and Kohn [1] is now known as a fundamental reference of the density functional theory. In this work, it is shown that the ground states energy of electrons is a unique functional of the electron density. Furthermore, given external potential, it is shown that the ground-state energy can be obtained by minimizing the energy functional, with respect to the electron density. When the density is the true ground-state electron density, this minimizes the energy functional. In a subsequent paper by Kohn and Sham [3], it is shown that the energy functional is recast by using orbitals as $E_{KS}(\{\Psi_i\})$ subjected to the orthogonalization condition of the set of one-electron wavefunctions $\Psi_i(r)$

$$\begin{aligned}
 E_{KS}(\{\Psi_i\}) &= -\frac{1}{2} \sum_i n_i \int \Psi_i \nabla^2 \Psi_i d^3 \mathbf{r} + \int \rho(\mathbf{r}) V_{ion}(\mathbf{r}) d^3 \mathbf{r} \\
 &+ \frac{e^2}{2} \int \frac{\rho(\mathbf{r}) \rho(\mathbf{r}')}{|\mathbf{r} - \mathbf{r}'|} d^3 \mathbf{r} d^3 \mathbf{r}' + E_{xc}[\rho(\mathbf{r})] + E_{ion}(\{\mathbf{R}_n\}). \quad (1.3)
 \end{aligned}$$

where E_{KS} is Kohn-Sham functional energy, the i -summation takes over all one-electron orbits, n_i the number of occupations in i -state, E_{xc} the exchange energy, and

$\rho(\mathbf{r})$ is the charge density and given by

$$\rho(\mathbf{r}) = \sum_i |\Psi_i(\mathbf{r})|^2. \quad (1.4)$$

The wavefunctions Ψ_i which minimize the Kohn-Sham functional energy in Eq.(1.3) satisfy the following eigenvalue equations,

$$H_{KS}\Psi_i = \epsilon_i\Psi_i, \quad (1.5)$$

where H_{KS} is Kohn-Sham's Hamiltonian,

$$H_{KS} = -\frac{1}{2}\nabla^2 + V_{ion}(\mathbf{r}) + V_H(\mathbf{r}) + V_{xc}(\mathbf{r}), \quad (1.6)$$

here, $V_H(r)$ is Hartree-Fock potential

$$V_H = \int \frac{\rho(\mathbf{r}')}{|\mathbf{r} - \mathbf{r}'|} d^3\mathbf{r}', \quad (1.7)$$

V_{xc} is exchange correlation potential

$$V_{xc}(\mathbf{r}) = \frac{\delta E_{xc}[\rho]}{\delta \rho(\mathbf{r})}, \quad (1.8)$$

and ϵ_i and Ψ_i denote the eigenvalues and eigenfunctions of the Kohn-Sham equation, respectively.

The wavefunctions calculated by Eq. (1.5) yield the charge density by Eq. (1.4), which is just $\rho(\mathbf{r})$ appearing in the Hartree-Fock and exchange potential. Hence, the Kohn-Sham equation must be solved self-consistently.

It seems that Eq. (1.5) plays a role of *Schrödinger* equation of one-electron wavefunction, but the thought underlying these equation is quite different. For the case of Hartree-Fock, the wavefunctions are treated as the most important quantity, and the charge density is second one, in other words, a dependent variable. On the other

hand, in the density functional theory, the charge density comes first. Wavefunctions are something expedient, so that they are allowed to vary as far as the charge density is the same. In the case of nanostructure of spherical symmetry density at the interior of the dot is uniform and density at the surface is not uniform.

1.1.1 Local Density Approximation

A price of mathematical simplification of the density functional method, which replaces the many-electronic problem by one-electron problem is paid by introducing unknown functional of exchange and correlation E_{xc} of the charge density. Fortunately, there is an easy approximation for E_{xc} . The most widely used form of E_{xc} is the so-called local density approximation (LDA). That is, the exchange and correlation energy of uniform electron gas, which is well studied, is used. In this approximation, the exchange-correlation energy at each point of the real space, E_{xc} , is assumed to be equal to that energy of a uniform electron gas with the same charge density.

$$E_{xc}[\rho] = \int \epsilon_{xc}(\mathbf{r})\rho(\mathbf{r})d^3\mathbf{r}, \quad (1.9)$$

where $V_{xc}(\mathbf{r})$ is exchange potential and given by,

$$V_{xc}(\mathbf{r}) = \frac{\delta E_{xc}}{\delta \rho(\mathbf{r})} = \frac{\partial(\rho(\mathbf{r})\epsilon_{xc}(\mathbf{r}))}{\partial \rho(\mathbf{r})}, \quad (1.10)$$

where $\epsilon_{xc}(\mathbf{r})$ is,

$$\epsilon_{xc}(\mathbf{r}) = \epsilon_{xc}^{hom}[\rho(\mathbf{r})], \quad (1.11)$$

where ϵ_{xc}^{hom} is the exchange-correlation energy in a uniform electron gas of that charge density. Actual form of the exchange and correlation energy as the function of the

charge density is constructed, based on the most reliable studies about homogeneous electron gas [3]. Within the local density approximation, the exchange and correlation potentials become a local function of the charge density. Tremendous of calculations for solids and molecules have shown effectiveness and accuracy of this approximation.

1.1.2 Pseudopotential Approximation

The second approximation which follows the local density approximation is use of pseudopotential. The wavefunctions of solid is expanded here through the set of plane waves. Plane-wave expansion it is uneconomical to describe localized states, such as core states of atoms which exhibit strong oscillations in the core region. Fortunately, the physical and chemical characteristics of many materials are governed by the valence electrons which extend to more wide region, and the core states are insensitive to those properties. We then can make an approximation by using valence electrons solely in describing the chemical combining characters of materials. Therefore, needed potentials have relatively slowly varying characters and this is desired properties. The wavefunctions which simulate the valence electrons accords to that are called the pseudo-wavefunctions. In this subsection, the procedure for constructing an ab initio pseudopotential within density functional theory will be illustrated. Using the approach Kohn and Sham [2], one can write down a Hamiltonian corresponding to a one-electron *Schrödinger* equation.

The pseudopotential are constructed so as they describe as much precisely as possible the electron scattering characters outside the core region. In general, pseudopotentials of an atom have different scattering characters in each angular momentum

and are nonlocal. Mathematically, pseudopotentials can be expressed as,

$$\hat{V}_{NL} = \sum_{\ell} |\ell m\rangle V_{\ell} \langle \ell m| \quad (1.12)$$

where $|\ell m\rangle$ is spherically harmonic functions, ℓ and m are the angular momentum, and the projected angular momentum, respectively. The original bare potential is of course a local potential. Because the true wavefunction and the pseudo-wavefunction are matched outside the core region, non-locality of pseudopotential is limited in the core region. Though many empirical potentials had been devised in the past to construct pseudopotentials, a great step had been achieved by introducing the concept "norm conservation" of wavefunction by Hamann [4]. As a result, it is not an exaggeration to say that pseudopotential method came to be used most generally today as a method to solve the problem of solid. In this procedure, a nodeless pseudo-wavefunction is initially taken so as to match to the true wavefunction outside core radius r_c . A norm-conserving condition, along with other conditions, the final form of potential is completed. The process is depicted in Fig. 1.1.

The pseudopotentials defined by expression (1.12) may be called semi-local one. The reason is that it is local for the radial element of the position, though it is nonlocal for the angle element. Kleinman and Bylander proposed the full-nonlocal type by which the radial element is treated nonlocal [5]. According to this, the potential is recast by

$$V_{ion} = V_L + \sum_{\ell m} \frac{|\Phi_{\ell m}^0 \Delta V_{\ell}\rangle \langle \Delta V_{\ell} \Phi_{\ell m}^0|}{\langle \Phi_{\ell m}^0 | \Delta V_{\ell} | \Phi_{\ell m}^0 \rangle}, \quad (1.13)$$

where $\Phi_{\ell m}^0$ is the pseudo-wavefunction of the atom when the pseudopotential is constructed. ΔV_{ℓ} is obtained by

$$\Delta V_{\ell} = V_{\ell,NL} - V_L, \quad (1.14)$$

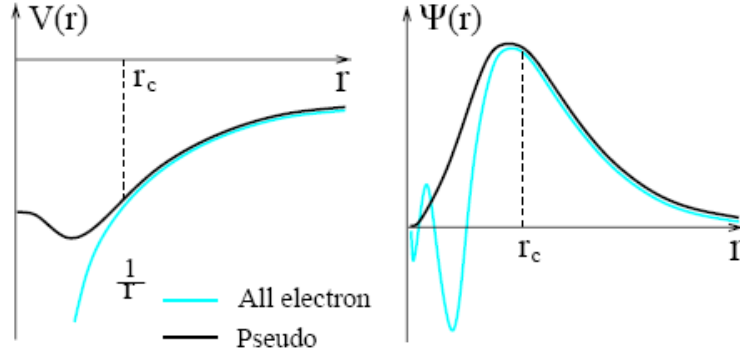


Figure 1.1: Schematic representation of a pseudopotential (left, dark curve) and a pseudo-wavefunction (right, dark curve) along with the all-electron potential (with the $1/r$ tail) and wavefunction (light curves). Notice that the all-electron and pseudo-functions are identical beyond the radial cutoff r_c and the pseudo-functions are smooth outside the core region.

Giving nonlocal potential in this way, the calculation of nonlocal part of the potential is greatly accelerated. Further benefit is obtained in calculation of operating of nonlocal potential onto wavefunctions if the arbitrariness of V_L is utilized.

In 1980, Kerker [6] proposed a straightforward method for constructing local density pseudopotentials that retained the norm conserving criterion. He suggested that the pseudo-wavefunction have the following form,

$$\phi_p(r) = r^\ell \exp(p(r)) \quad \text{for } r < r_c, \quad (1.15)$$

where $p(r)$ is a simple polynomial: $p(r) = -a_0 r^4 - a_1 r^3 - a_2 r^2 - a_3$ and

$$\phi_p(r) = \psi_{AE}(r) \quad \text{for } r > r_c. \quad (1.16)$$

This form of the pseudo-wavefunction for ϕ_p assures that the function will be nodeless and have the correct behavior at large r . Kerker proposed a criteria for fixing the parameters (a_0, a_1, a_2 and a_3). One criteria is that the wavefunction be norm

conserving. Other criteria include: (a) The all electron and pseudo-wavefunctions have the same valence eigenvalue. (b) The pseudo-wavefunction be nodeless and be identical to the all-electron wavefunction for $r > r_c$. (c) The pseudo-wavefunction must be continuous as well as the first and second derivatives of the wavefunction at r_c .

Once the pseudo-wavefunction is defined as in Eqs. (1.15) and (1.16) we can invert the Kohn-Sham equation and solve for the ion core pseudopotential, $V_{ion,p}$:

$$V_{ion,p}^n(\vec{r}) = E_n - V_H(\vec{r}) - V_{xc}[\vec{r}, \rho(\vec{r})] + \frac{\hbar^2 \nabla^2 \phi_{p,n}}{2m\phi_{p,n}}, \quad (1.17)$$

This potential, when self-consistently screened by the pseudo-charge density:

$$\rho(\vec{r}) = -e \sum_{n,occup} |\phi_{p,n}(\vec{r})|^2, \quad (1.18)$$

will yield the eigenvalue of E_n and a pseudo-wavefunction $\phi_{p,n}$. The pseudo-wavefunction by construction will agree with the all electron wavefunction away from the core.

In our study the important issue to consider for nanosilicon is about the details of this construction. First, the potential is state dependent as written in Eq. (1.17), i.e., the pseudopotential is dependent on the quantum state n . This issue can be handled by recognizing the non-locality of the pseudopotential. Since the core potential is highly bound, the ion core potential is highly localized and is not sensitive to the ground state configuration used to compute the pseudopotential. This pseudopotential should converge to the all electron potential outside of the core.

1.2 Time-dependent Density Functional Theory

DFT, reviewed in the previous section, is usually addressed as a ground-state theory. This is inexact: the excited states are also uniquely determined by the

ground-state density, i.e. the excitation energies, for example, are also functionals of the ground state density. Unfortunately these functionals are unknown. Note that Hohenberg-Kohn theorem is an existence statement and it does not provide with a constructive procedure for the functionals. However, our approach to the study of the electronic excited states is based on yet another extension: time-dependent local density approximation (TDLDA). Note that TDDFT is the extension of DFT to time-dependent phenomena. It allows for the calculation of excitations, but its scope is larger, since in fact, it is an exact reformulation of the time-dependent *Schrödinger* equation. In the following, we will shallowly review the foundations of the theory.

TDDFT is based on the Runge-Gross theorem [2] which states that, given initial state at t_o , the single particle potential $v(\mathbf{r}, t)$ leading to a given density $\rho(\mathbf{r}, t)$ is uniquely determined so that the map $v(\mathbf{r}, t) \rightarrow \rho(\mathbf{r}, t)$ is invertible. As a consequence of the bijective map $v(\mathbf{r}, t) \leftrightarrow \rho(\mathbf{r}, t)$, every observable $O(t)$ is unique functional of, and can be calculated from, the density $\rho(\mathbf{r}, t)$.

Note that in this case: (i) Two potentials are considered equivalent if they differ by any purely time-dependent function (because then they produce wavefunctions which are equal up to purely time-dependent phase, which is cancelled when any observable is calculated from them), and (ii) There is a dependence on the initial quantum state of the system. (iii) It was shown that under very broad assumptions a time-dependent one-body potential $v_{KS}(\mathbf{r}, t)$ exists that produces a given smooth density $\rho(\mathbf{r}, t)$ at all times. Of course, we need to still need to assume that the initial state is, noninteracting v-representable.

Armed with the Runge-Gross (RG) theorem, and in a similar way to the Kohn-Sham construction for the ground state density, we may build a time-dependent

Kohn-Sham scheme. For that purpose, we have to introduce an auxiliary system of N noninteracting electrons, subject to an external potential v_{KS} . This potential is unique, by virtue of Runge-Gross theorem applied to the noninteracting system, and is chosen such that the density of the Kohn-Sham electrons is the same as the density of the original interacting system. These Kohn-Sham electrons obey the time-dependent *Schrödinger* equation

$$i\frac{\partial}{\partial t}\Psi_j(\mathbf{r}, t) = \hat{H}(\mathbf{r}, t)\Psi_j(\mathbf{r}, t), \quad (1.19)$$

where the Kohn-Sham Hamiltonian is defined as

$$\hat{H}_{KS}(\mathbf{r}, t) = -\frac{\nabla^2}{2} + v_{KS}[\rho](\mathbf{r}, t). \quad (1.20)$$

Thus, the time-dependent form of a self-consistent single particle equation becomes

$$\left\{ \hat{H}_{KS}(\mathbf{r}, t) = -\frac{\nabla^2}{2} + v_{KS}[\rho](\mathbf{r}, t) \right\} \Psi_j(\mathbf{r}, t) = i\frac{\partial}{\partial t}\Psi_j(\mathbf{r}, t) \quad (1.21)$$

By construction, the density of the interacting system can be calculated from the Kohn-Sham orbitals

$$\rho(\mathbf{r}, t) = \sum_{j=1}^N \Psi_j^\dagger(\mathbf{r}, t)\Psi_j(\mathbf{r}, t). \quad (1.22)$$

As in the Kohn-Sham scheme for the ground state, the time-dependent Kohn-Sham potential is normally written as the sum of three terms

$$v_{KS}[\rho](\mathbf{r}, t) = v_{ext}(\mathbf{r}, t) + V_H[\rho](\mathbf{r}, t) + V_{xc}[\rho](\mathbf{r}, t). \quad (1.23)$$

The first term is the external potential, whereas the second accounts for the classical electrostatic interaction between electrons

$$V_H[\rho] = \int d^3\mathbf{r}' \frac{\rho(\mathbf{r}', t)}{|\mathbf{r} - \mathbf{r}'|}. \quad (1.24)$$

The third term, the exchange correlation potential includes all the nontrivial many-body effects, and has an extremely complex (and essentially unknown) functional dependence on the density. This dependence is clearly nonlocal, both in space and in time, that is, the potential at all other positions \mathbf{r} can depend on the density at all other positions and previous times.

In the adiabatic approximation, which is local in time, the exchange-correlation potential and its first derivative can be expressed in terms of the time-independent exchange-correlation energy, $E_{xc}[\rho]$,

$$v_{xc}[\rho(\mathbf{r}, t)] \cong \frac{\delta E_{xc}[\rho]}{\delta \rho(\mathbf{r})}, \quad (1.25)$$

$$\frac{\delta v_{xc}[\rho(\mathbf{r}, t)]}{\delta \rho(\mathbf{r}', t')} \cong \delta(t - t') \frac{\delta^2 E_{xc}[\rho]}{\delta \rho(\mathbf{r}) \delta \rho(\mathbf{r}')}. \quad (1.26)$$

The LDA makes a separate local approximation, i.e., within the LDA, the exchange-correlation energy density is local in space. The local density approximation in time dependent density functional theory interestingly agrees with experimental investigations.

Chapter 2

Time Dependent Density Functional Based Linear Response Theory

In this chapter we will derive the general equations of TDDFT-based linear response theory, necessary for photo-absorption calculations in silicon nanocrystallites.

2.1 Time Dependent Response Theory

The linear response formalism within TDDFT provides a theoretical basis for the TDLDA excitation energies and oscillator strengths which are derived from the single-electron Kohn-Sham eigenvalues and eigenfunctions. The response of the Kohn-Sham density matrix within TDDFT is obtained by introducing a time-dependent perturbation $\delta v_{appl}(\mathbf{r}, t)$. Due to the self consistent nature of the Kohn-Sham Hamiltonian, the effective perturbation includes the response of the self-consistent field. Consider a basis set of time-independent orthonormal spin-orbits $\psi_{i\sigma}$, where i and σ refer to space and spin indices respectively. These orbitals are the molecular orbitals of the unperturbed system. The corresponding annihilation operators are $\hat{a}_{i\sigma}$.

The linear response of the applied field is

$$\delta\hat{v}_{appl}(t) = \sum_{ij\sigma} \delta v_{ij\sigma}^{appl}(t) \hat{a}_{i\sigma}^\dagger \hat{a}_{j\sigma}. \quad (2.1)$$

The density matrix is given by $P_{ij\sigma}(t) = \langle \Psi_0(t) | \hat{a}_{j\sigma}^\dagger \hat{a}_{i\sigma} | \Psi_0(t) \rangle$ and hence its linear response is

$$\delta P_{ij\sigma}(t) = \langle \delta \Psi_0(t) | \hat{a}_{j\sigma}^\dagger \hat{a}_{i\sigma} | \Psi_0(t) \rangle + \langle \Psi_0(t) | \hat{a}_{j\sigma}^\dagger \hat{a}_{i\sigma} | \delta \Psi_0(t) \rangle, \quad (2.2)$$

which is conveniently expressed in terms of the generalized susceptibility as

$$\delta P_{ij\sigma}(t) = \sum_{k\ell\tau} \int_{-\infty}^{\infty} \chi_{ij\sigma, k\ell\tau}(t-t') \delta v_{k\ell\tau}^{appl}(t') dt'. \quad (2.3)$$

Introducing the Fourier transform convention

$$f(\omega) = \int_{-\infty}^{\infty} e^{i\omega t} f(t) dt, \quad f(t) = \frac{1}{2\pi} \int_{-\infty}^{\infty} e^{-i\omega t} f(\omega) d\omega, \quad (2.4)$$

and making use of the convolution theorem

$$h(t) = \int_{-\infty}^{\infty} g(t-t') f(t') dt' \iff h(\omega) = g(\omega) f(\omega), \quad (2.5)$$

allows Eq.(2.3) to be rewritten as

$$\delta P_{ij\sigma}(\omega) = \sum_{k\ell\tau} \chi_{ij\sigma, k\ell\tau}(\omega) \delta v_{k\ell\tau}^{appl}(\omega) \quad (2.6)$$

2.1.1 Derivation of Generalized Susceptibility

To derive a formula for the generalized susceptibility, assume that the system is initially in its ground stationary state Ψ_0 , and introduce a perturbation

$$\delta\hat{w}(t) = e^{-\eta(t_1-t)} \delta\hat{v}_{appl}(t), \quad (2.7)$$

where η is a positive infinitesimal such that $\delta w(t_1) = \delta v(t_1)$. From standard time-dependent perturbation theory we know that

$$|\delta\Psi_0(t_1)\rangle = -i \sum_{I \neq 0} |\Psi_I(t_1)\rangle \int_{-\infty}^{t_1} \langle \Psi_I(t) | \delta\hat{w}(t) | \Psi_0(t) \rangle dt, \quad (2.8)$$

where $\Psi_I(t) = e^{-E_I t} \Psi_I$ are the stationary states of the unperturbed Hamiltonian.

$$\begin{aligned} |\delta\Psi_0(t_1)\rangle &= -i \sum_{I \neq 0} |\Psi_I(t_1)\rangle \int_{-\infty}^{t_1} \langle \exp\{iE_I t\} \Psi_I | \delta\hat{w}(t) | \exp\{-iE_0 t\} \Psi_0 \rangle dt, \\ &= -i \sum_{I \neq 0} \int_{-\infty}^{t_1} |\Psi_I(t_1)\rangle \langle \Psi_I | \delta\hat{v}_{appl} | \Psi_0 \rangle \\ &\quad \exp\{-iE_I(t_1 - t) - iE_0 t - \eta(t_1 - t)\} dt, \end{aligned} \quad (2.9)$$

Taking the complex conjugate of the above equation we have,

$$\langle \delta\Psi_0(t_1) | = i \sum_{I \neq 0} \int_{-\infty}^{t_1} \langle \Psi_I | \langle \Psi_I | \delta\hat{v}_{appl} | \Psi_0 \rangle \exp\{iE_I(t_1 - t) + iE_0 t - \eta(t_1 - t)\} dt, \quad (2.10)$$

Then, the linear response of the density matrix at time t_1 is

$$\begin{aligned} \delta P_{ij\sigma}(t_1) &= \langle \delta\Psi_0(t_1) | \hat{a}_{j\sigma}^\dagger \hat{a}_{i\sigma} | \Psi_0(t_1) \rangle + \langle \Psi_0(t_1) | \hat{a}_{j\sigma}^\dagger \hat{a}_{i\sigma} | \delta\Psi_0(t_1) \rangle \\ &= i \sum_{I \neq 0} \int_{-\infty}^{t_1} \left[\langle \Psi_I | \hat{a}_{j\sigma}^\dagger \hat{a}_{i\sigma} | \Psi_0 \exp\{-iE_0 t_1\} \rangle \langle \Psi_0 | \sum_{k\ell\tau} \delta v_{k\ell\tau}^{appl} \hat{a}_{k\tau}^\dagger \hat{a}_{\ell\tau} | \Psi_I \rangle \right. \\ &\quad \exp\{iE_I(t_1 - t) + iE_0 t - \eta(t_1 - t)\} - i \langle \Psi_0 \exp\{iE_0 t_1\} | \hat{a}_{k\tau}^\dagger \hat{a}_{\ell\tau} | \Psi_I \rangle \\ &\quad \left. \langle \Psi_I | \sum_{k\ell\tau} \delta v_{k\ell\tau}^{appl} \hat{a}_{j\sigma}^\dagger \hat{a}_{i\sigma} | \Psi_0 \rangle \exp\{-iE_I(t_1 - t) - iE_0 t - \eta(t_1 - t)\} \right] dt, \end{aligned} \quad (2.11)$$

$$\begin{aligned} \delta P_{ij\sigma} &= \sum_{k\ell\tau} \int_{-\infty}^{\infty} \left\{ -i\Theta(t_1 - t) \sum_{I \neq 0} \left[\langle \Psi_0 | \hat{a}_{j\sigma}^\dagger \hat{a}_{i\sigma} | \Psi_I \rangle \langle \Psi_I | \hat{a}_{k\tau}^\dagger \hat{a}_{\ell\tau} | \Psi_0 \rangle \right. \right. \\ &\quad \left. \exp\{-i(E_I - E_0 - i\eta)(t_1 - t)\} \right. \\ &\quad \left. \left. - \langle \Psi_0 | \hat{a}_{k\tau}^\dagger \hat{a}_{\ell\tau} | \Psi_I \rangle \langle \Psi_I | \hat{a}_{j\sigma}^\dagger \hat{a}_{i\sigma} | \Psi_0 \rangle \exp\{-i(E_0 - E_I - i\eta)(t_1 - t)\} \right] \right\} \delta v_{k\ell\tau}^{appl} dt, \end{aligned} \quad (2.12)$$

where

$$\Theta(t_1 - t) = \begin{cases} 1 & \text{for } t_1 > t \\ 0 & \text{for } t_1 < t \end{cases},$$

is the heaviside function. Now, comparing Eq.(2.6)and Eq.(2.12)we have,

$$\begin{aligned} \chi_{ij\sigma,k\ell\tau} &= -i\Theta(t_1 - t) \sum_{I \neq 0} \left[\langle \Psi_0 | \hat{a}_{j\sigma}^\dagger \hat{a}_{i\sigma} | \Psi_I \rangle \langle \Psi_I | \hat{a}_{k\tau}^\dagger \hat{a}_{\ell\tau} | \Psi_0 \rangle \exp\{-i(E_I - E_0 - i\eta)(t_1 - t)\} \right. \\ &\quad \left. - \langle \Psi_0 | \hat{a}_{k\tau}^\dagger \hat{a}_{\ell\tau} | \Psi_I \rangle \langle \Psi_I | \hat{a}_{j\sigma}^\dagger \hat{a}_{i\sigma} | \Psi_0 \rangle \exp\{-i(E_0 - E_I - i\eta)(t_1 - t)\} \right]. \end{aligned} \quad (2.13)$$

Thus, taking the Fourier transform of the above equation gives the sum-over-state (SOS) representation of the generalized susceptibility,

$$\chi_{ij\sigma,k\ell\tau} = \sum_{I \neq 0} \left[\frac{\langle \Psi_0 | \hat{a}_{j\sigma}^\dagger \hat{a}_{i\sigma} | \Psi_I \rangle \langle \Psi_I | \hat{a}_{k\tau}^\dagger \hat{a}_{\ell\tau} | \Psi_0 \rangle}{\omega - (E_I - E_0) + i\eta} - \frac{\langle \Psi_0 | \hat{a}_{k\tau}^\dagger \hat{a}_{\ell\tau} | \Psi_I \rangle \langle \Psi_I | \hat{a}_{j\sigma}^\dagger \hat{a}_{i\sigma} | \Psi_0 \rangle}{\omega + (E_I - E_0) + i\eta} \right]. \quad (2.14)$$

If a single particle system is initially in orbital $\psi_{m\mu}$ and the unperturbed stationary states are taken as the orthonormal basis set, then Eq.(2.14) can be written as

$$\begin{aligned} \chi_{ij\sigma,k\ell\tau} &= \sum_{I \neq 0} \left[\frac{\langle \Psi_{m\mu} | \hat{a}_{j\sigma}^\dagger \hat{a}_{i\sigma} | \Psi_I \rangle \langle \Psi_I | \hat{a}_{k\tau}^\dagger \hat{a}_{\ell\tau} | \Psi_{m\mu} \rangle}{\omega - (E_I - E_0) + i\eta} - \frac{\langle \Psi_{m\mu} | \hat{a}_{k\tau}^\dagger \hat{a}_{\ell\tau} | \Psi_I \rangle \langle \Psi_I | \hat{a}_{j\sigma}^\dagger \hat{a}_{i\sigma} | \Psi_{m\mu} \rangle}{\omega + (E_I - E_0) + i\eta} \right] \\ &= \delta_{\sigma,\tau} \delta_{\sigma,\mu} \delta_{i,k} \delta_{j,\ell} \frac{\delta_{j,m} - \delta_{i,m}}{\omega - (\epsilon_{i\sigma} - \epsilon_{j\sigma})}. \end{aligned} \quad (2.15)$$

Since the response of the density matrix of systems of N independent particles with (possibly fractional) occupation numbers $n_{i\sigma}$ is the occupation number weighted sum of the response of the density matrices for the individual orbitals, assuming that no change in occupation number is induced by the perturbation, the generalized susceptibility can be rewritten as

$$\begin{aligned} \chi_{ij\sigma,k\ell\tau}(\omega) &= \sum_{m\mu} n_{m\mu} \delta_{\sigma,\tau} \delta_{\sigma,\mu} \delta_{i,k} \delta_{j,\ell} \frac{\delta_{j,m} - \delta_{i,m}}{\omega - (\epsilon_{i\sigma} - \epsilon_{j\sigma})} \\ &= \delta_{\sigma,\tau} \delta_{\sigma,\mu} \delta_{j,\ell} \frac{n_{j\sigma} - n_{i\sigma}}{\omega - (\epsilon_{i\sigma} - \epsilon_{j\sigma})} \end{aligned} \quad (2.16)$$

This is a generic expression for nano-clusters that we derived for arbitrary number of atoms with no overall symmetry. However, this expression will be modified when overall symmetry and surface passivations are incorporated.

2.2 Linear Response of the Density Matrix

The perturbation induced into the Kohn-Sham hamiltonian by turning on an applied field $\delta v_{eff}^\sigma(\mathbf{r}, t)$ is, to linear order,

$$\delta v_{eff}^\sigma(\mathbf{r}, t) = \delta v_{appl}(\mathbf{r}, t) + \delta v_{SCF}^\sigma(\mathbf{r}, t), \quad (2.17)$$

where the self-consistent field is the sum of Hartree and exchange-correlation potential,

$$v_{SCF}^\sigma(\mathbf{r}, t) = \int \frac{\rho_v(\mathbf{r}, t)}{|\mathbf{r} - \mathbf{r}'|} d\mathbf{r}' + v_{xc}[\rho](\mathbf{r}, t), \quad (2.18)$$

is the linear response of the self-consistent field arising from the change in the charge density. Thus the quasi-independent particle nature of the Kohn-Sham equation means that the independent particle nature of the generalized susceptibility Eq.(2.16), can be used together with the perturbation $\delta v_{eff}^\sigma(\mathbf{r}, t)$ to write down the linear response of the Kohn-Sham density matrix to the applied field. In the basis of the unperturbed molecular orbitals,

$$\delta P_{ij\sigma}(\omega) = \sum_{kl\tau} \chi_{ij\sigma,kl\tau}(\omega) \delta v_{kl\tau}^{eff} = \frac{n_{j\sigma} - n_{i\sigma}}{\omega - (\epsilon_{i\sigma} - \epsilon_{j\sigma})} \delta v_{ij\sigma}^{eff}(\omega). \quad (2.19)$$

The previous equation is however, complicated by the fact that $\delta v_{ij\sigma}^{SCF}(\omega)$ depends on the response of the density matrix,

$$\begin{aligned} \delta v_{ij\sigma}^{SCF}(\omega) &= \sum_{kl\tau} \frac{\partial v_{ij\sigma}^{SCF}}{\partial P_{kl\tau}} \delta P_{kl\tau} \\ &= \sum_{kl\tau} K_{ij\sigma,kl\tau} \delta P_{kl\tau}, \end{aligned} \quad (2.20)$$

where the coupling matrix, $K_{ij\sigma,k\ell\tau}(t) = \frac{\partial v_{ij\sigma}^{SCF}(t)}{\partial P_{k\ell\tau}(t)}$, describes the response the self-consistent field to changes in the charge density. Taking the Fourier transform of the coupling matrix we get,

$$\begin{aligned}
K_{ij\sigma,k\ell\tau}(\omega) &= \int_{-\infty}^{\infty} \exp\{+i\omega(t-t')\} \frac{\partial v_{ij\sigma}^{SCF}(t)}{\partial P_{k\ell\tau}(t')} d(t-t'), \\
&= \int_{-\infty}^{\infty} \exp\{i\omega(t-t')\} \left\{ \sum_{\mu} \int \int \frac{\delta v_{ij\sigma}^{SCF}(t)}{\delta \rho_{\mu}(\mathbf{r}, t'')} \frac{\partial \rho_{\mu}(\mathbf{r}, t'')}{\partial P_{k\ell\tau}(t')} d\mathbf{r} dt'' \right\} d(t-t'), \\
&= \int \int \Psi_{i\sigma}^*(\mathbf{r}) \Psi_{j\sigma}(\mathbf{r}) \frac{1}{|\mathbf{r}-\mathbf{r}'|} \Psi_{k\tau}(\mathbf{r}') \Psi_{\ell\tau}^*(\mathbf{r}') + \left\{ \int_{-\infty}^{\infty} \exp\{+i\omega(t-t')\} \right. \\
&\quad \left. \int \int \Psi_{i\sigma}^*(\mathbf{r}) \Psi_{j\sigma}(\mathbf{r}) \frac{\delta^2 E_{xc}[\rho]}{\delta \rho_{\sigma}(\mathbf{r}, t) \delta \rho_{\tau}(\mathbf{r}', t')} \Psi_{k\tau}(\mathbf{r}') \Psi_{\ell\tau}^*(\mathbf{r}') d\mathbf{r} d\mathbf{r}' \right\} d(t-t'), \\
&= \int \int \Psi_{i\sigma}^*(\mathbf{r}) \Psi_{j\sigma}(\mathbf{r}) \left\{ \frac{1}{|\mathbf{r}-\mathbf{r}'|} + \frac{\delta^2 E_{xc}[\rho]}{\delta \rho_{\sigma}(\mathbf{r}) \delta \rho_{\tau}(\mathbf{r}')} \right\} \Psi_{k\tau}(\mathbf{r}') \Psi_{\ell\tau}^*(\mathbf{r}') d\mathbf{r} d\mathbf{r}', \quad (2.21)
\end{aligned}$$

where the functional derivative is evaluated using the unperturbed spin-up and spin-down charge densities. Using Eqs.(2.17), (2.20) and (2.21), Eq.(2.19) can be written as

$$\delta P_{ij\sigma}(\omega) = \frac{n_{j\sigma} - n_{i\sigma}}{\omega - (\epsilon_{i\sigma} - \epsilon_{j\sigma})} \left[\delta v_{ij\sigma}^{appl}(\omega) + \sum_{k\ell\tau} K_{ij\sigma,k\ell\tau}(\omega) \delta P_{k\ell\tau}(\omega) \right], \quad (2.22)$$

rearranging the above equation we get

$$\sum_{k\ell\tau}^{n_{k\tau} - n_{\ell\tau} \neq 0} \left[\delta_{\sigma,\tau} \delta_{i,k} \delta_{j,\ell} \frac{\omega - (\epsilon_{k\sigma} - \epsilon_{\ell\sigma})}{n_{\ell\tau} - n_{k\tau}} - K_{ij\sigma,k\ell\tau}(\omega) \right] \delta P_{k\ell\tau}(\omega) = \delta v_{ij\sigma}^{appl}(\omega), \quad (2.23)$$

where $n_{k\tau} \neq n_{\ell\tau}$. Solving the above equation for $\delta P(\omega)$ then allows response properties to be calculated. From Eq.(2.21) we see that the coupling matrix satisfies the following relation:

1.

$$K_{ij\sigma,k\ell\tau}(\omega) = [K_{k\ell\tau,ij\sigma}(\omega)]^*. \quad (2.24)$$

2. When the molecular orbitals are real,

$$K_{ij\sigma,kl\tau}(\omega) = K_{ij\sigma,lk\tau}(\omega) = K_{ji\sigma,kl\tau}(\omega) = K_{ji\sigma,kl\tau}(\omega). \quad (2.25)$$

3. In the adiabatic approximation, the replacement $\frac{\delta E_{xc}}{\delta\rho_\sigma(\mathbf{r},t)\delta\rho_\tau(\mathbf{r}',t')} \rightarrow \delta(t-t')\frac{\delta E_{xc}}{\delta\rho_\sigma(\mathbf{r})\delta\rho_\tau(\mathbf{r}'')}$

results in a coupling matrix which is no longer a function of ω , and which is real when the molecular orbitals are real. And hence K is hermitian,

$$K_{ij\sigma,kl\tau} = K_{ji\sigma,kl\tau}^* \quad (2.26)$$

Furthermore, K is real when molecular orbitals are real, but even in this case

$$K_{ij\sigma,kl\tau} \neq K_{ij\sigma,kl\tau}. \quad (2.27)$$

Since only the particle-hole $n_{i\sigma} > n_{j\sigma}$, and hole-particle, $n_{i\sigma} < n_{j\sigma}$, elements $\delta P_{ij\sigma}$ of the response of the density matrix are nonzero it is convenient to treat only these elements and divide $\delta P_{ij\sigma}$ into particle-hole and hole-particle parts.

We start by ordering the orbital basis $\Psi_{i\sigma}$ such that $i < j \leftrightarrow n_{i\sigma} \geq n_{j\sigma}$. Now consider $n_{i\sigma} > n_{j\sigma}$. Then the $\delta P_{ij\sigma}$ are the particle-hole matrix elements and $\delta P_{ji\sigma}$ are the hole-particle matrix elements, and can be written as two separate equations, the first giving the particle-hole part of δv^{appl} ,

$$\left\{ \sum_{kl\tau}^{n_{k\tau}-n_{l\tau}>0} \left[\delta_{\sigma,\tau} \delta_{i,k} \delta_{j,l} \frac{\omega - (\epsilon_{k\tau} - \epsilon_{l\tau})}{n_{l\tau} - n_{k\tau}} - K_{ij\sigma,kl\tau}(\omega) \right] \delta P_{kl\tau}(\omega) - \sum_{kl\tau}^{n_{k\tau}-n_{l\tau}>0} K_{ij\sigma,kl\tau}(\omega) \delta P_{kl\tau}(\omega) \right\} = \delta v_{ij\sigma}^{appl}(\omega), \quad (2.28)$$

and the second giving the hole-particle part of $\delta v^{appl}(\omega)$,

$$\left\{ \sum_{kl\tau}^{n_{k\tau}-n_{l\tau}>0} \left[\delta_{\sigma,\tau} \delta_{i,k} \delta_{j,l} \frac{\omega - (\epsilon_{l\tau} - \epsilon_{k\tau})}{n_{k\tau} - n_{l\tau}} - K_{ji\sigma,kl\tau}(\omega) \right] \delta P_{kl\tau}(\omega) - \sum_{kl\tau}^{n_{k\tau}-n_{l\tau}>0} K_{ji\sigma,kl\tau}(\omega) \delta P_{kl\tau}(\omega) \right\} = \delta v_{ji\sigma}^{appl}(\omega), \quad (2.29)$$

If the molecular orbitals are real, using the symmetry property in Eq.(2.27), we can combine Eqs.(2.28) and (2.29) into a single matrix equation as,

$$\left[\begin{pmatrix} \mathbf{A}(\omega) & \mathbf{B}(\omega) \\ \mathbf{B}(\omega) & \mathbf{A}(\omega) \end{pmatrix} - \omega \begin{pmatrix} \mathbf{C} & 0 \\ 0 & -\mathbf{C} \end{pmatrix} \right] \begin{pmatrix} \delta \mathbf{P}(\omega) \\ \delta \mathbf{P}^*(\omega) \end{pmatrix} = \begin{pmatrix} \delta \mathbf{v}_{appl}(\omega) \\ \delta \mathbf{v}_{appl}^*(\omega) \end{pmatrix}, \quad (2.30)$$

where:

$$\begin{aligned} \mathbf{A}_{ij\sigma,kl\tau}(\omega) &= \delta_{\sigma,\tau} \delta_{i,k} \delta_{j,\ell} \frac{\epsilon_{k\tau} - \epsilon_{\ell\tau}}{n_{k\tau} - n_{\ell\tau}} - K_{ij\sigma,kl\tau}(\omega), \\ \mathbf{B}_{ij\sigma,kl\tau}(\omega) &= -K_{ji\sigma,\ell k\tau}(\omega), \\ \mathbf{C}_{ij\sigma,kl\tau} &= \frac{\delta_{\sigma,\tau} \delta_{i,k} \delta_{j,\ell}}{n_{k\tau} - n_{\ell\tau}}. \end{aligned}$$

Here, $\delta \mathbf{P}(\omega)$ denotes the Fourier transform of $\delta \mathbf{P}(t)$ (so $\delta \mathbf{P}_{\ell k\tau}(\omega) = \delta \mathbf{P}_{k\ell\tau}^*(\omega)$) and similarly for $\delta \mathbf{v}_{appl}^*(\omega)$. Note that in each block, the rows are labelled by $ij\sigma$ with $n_{i\sigma} > n_{j\sigma}$ and the columns are labelled by $kl\tau$ with $n_{k\tau} > n_{\ell\tau}$.

A suitable unitary transformation of Eq.(2.30) gives

$$\left[\begin{pmatrix} \mathbf{A}(\omega) + \mathbf{B}(\omega) & 0 \\ 0 & \mathbf{B}(\omega) + \mathbf{A}(\omega) \end{pmatrix} - \omega \begin{pmatrix} -\mathbf{C} & 0 \\ 0 & -\mathbf{C} \end{pmatrix} \right] \begin{pmatrix} \Re \delta \mathbf{P}(\omega) \\ -i \Im \delta \mathbf{P}^*(\omega) \end{pmatrix} = \begin{pmatrix} \Re \delta \mathbf{v}_{appl}(\omega) \\ -i \Im \delta \mathbf{v}_{appl}^*(\omega) \end{pmatrix} \quad (2.31)$$

This can be used to obtain the real and imaginary parts of $\delta \mathbf{P}$,

$$[[\mathbf{A}(\omega) - \mathbf{B}(\omega)] - \omega^2 \mathbf{C} [\mathbf{A}(\omega) - \mathbf{B}(\omega)]^{-1} \mathbf{C}] (\Im \delta \mathbf{P})(\omega) = \Im \delta \mathbf{v}_{appl}(\omega) \quad (2.32)$$

and for the real part

$$-i\omega \mathbf{C} [\mathbf{A}(\omega) + \mathbf{B}(\omega)]^{-1} (\Re \delta \mathbf{P}_{kl\tau})(\omega) = \Re \delta \mathbf{v}_{appl}(\omega) \quad (2.33)$$

For real perturbations, the real part of the response of the density matrix is given

by

$$\begin{aligned}
 & \sum_{k\ell\tau}^{n_{k\tau}-n_{\ell\tau}>0} \left\{ \delta_{k\ell}\delta_{i,k}\delta_{j,\ell} \frac{\epsilon_{k\sigma} - \epsilon_{\ell\tau}}{n_{k\tau} - n_{\ell\tau}} - 2K_{ij\sigma,k\ell\tau}(\omega) \right. \\
 & \left. - \omega^2 \frac{\delta_{\sigma,\tau}\delta_{i,k}\delta_{j,\ell}}{(n_{k\ell} - n_{\ell,\tau})(\epsilon_{k\tau} - \epsilon_{\ell\tau})} \right\} (\Re\delta P_{k\ell\tau})(\omega) = \delta v_{ij\sigma}^{appl}(\omega) \quad (2.34)
 \end{aligned}$$

In the following chapter, we use this equation to exploit the optical properties of hydrogenated silicon quantum dots.

Chapter 3

Results for Excitation Energies and Optical Gap

The interaction of a molecule with light can be modelled as the interaction with an electric field varying sinusoidally in time. Excitation energies and oscillator strengths can then be obtained from the poles and residues of the dynamic polarizability. These quantities are experimentally measurable one from spectroscopic data and has applied interest for nano-photonics applications.

3.1 Calculation of Excitation Energies and Oscillator Strength

The dynamic polarizability can be obtained by introducing a perturbation

$$\delta v_{\text{appl}}(t) = \hat{\gamma} \varepsilon_{\gamma}(t) \quad \gamma = \{x, y, z\}, \quad (3.1)$$

and expanding the $\hat{\gamma}$ component of the dipole moment to first order in the function $\varepsilon_{\gamma}(t)$, we have

$$\mu_{\beta}(t) = \mu_{\beta} + \int_{-\infty}^{\infty} \alpha_{\gamma\beta}(t-t') \varepsilon_{\gamma}(t') dt' + \dots \quad \beta = \{x, y, z\}, \quad (3.2)$$

where the first term on the right hand side refers to the permanent dipole moment.

Then, using the convolution theorem we get

$$\alpha_{\beta\gamma}(\omega) = \frac{\delta\mu_{\beta}(\omega)}{\varepsilon_{\gamma}(\omega)}, \quad (3.3)$$

where $\delta\mu_{\beta}(\omega)$ is the linear response of the dipole moment.

Since

$$\delta\mu_{\beta}(\omega) = - \sum_{ij\sigma} \beta_{ji\sigma} \delta P_{ij\sigma} = - \sum_{ij\sigma, k\ell\tau} \beta_{ji\sigma} \chi_{ij\sigma, k\ell\tau}(\omega) \gamma_{k\ell\tau} \varepsilon_{\gamma}(\omega), \quad (3.4)$$

It follows that

$$\alpha_{\beta\gamma}(\omega) = - \sum_{ij\sigma, k\ell\tau} \beta_{ji\sigma} \chi_{ij\sigma, k\ell\tau}(\omega) \gamma_{k\ell\tau}. \quad (3.5)$$

Using Eq.(2.14), Eq.(3.5) can be written as,

$$\begin{aligned} \alpha_{\beta\gamma}(\omega) &= - \sum_{ij\sigma, k\ell\tau} \beta_{ji\sigma} \left[\sum_I \frac{\langle \Psi_0 | \hat{a}_{j\sigma}^{\dagger} \hat{a}_{i\sigma} | \Psi_I \rangle \langle \Psi_I | \hat{a}_{\ell\tau}^{\dagger} \hat{a}_{k\tau} | \Psi_0 \rangle}{\omega - (E_I - E_0)} \right. \\ &\quad \left. - \frac{\langle \Psi_I | \hat{a}_{\ell\tau}^{\dagger} \hat{a}_{k\tau} | \Psi_0 \rangle \langle \Psi_0 | \hat{a}_{j\sigma}^{\dagger} \hat{a}_{i\sigma} | \Psi_I \rangle}{\omega + (E_I - E_0)} \right] \gamma_{k\ell\tau} \\ &= - \sum_I \left\{ \frac{\langle \Psi_I | \hat{\beta} | \Psi_0 \rangle \langle \Psi_0 | \hat{\gamma} | \Psi_I \rangle}{\omega - (E_I - E_0)} - \frac{\langle \Psi_I | \hat{\gamma} | \Psi_0 \rangle \langle \Psi_0 | \hat{\beta} | \Psi_I \rangle}{\omega + (E_I - E_0)} \right\} \end{aligned} \quad (3.6)$$

Using the fact that $\langle \Psi_I | \hat{\beta} | \Psi_0 \rangle \langle \Psi_0 | \hat{\gamma} | \Psi_I \rangle = \langle \Psi_I | \hat{\gamma} | \Psi_0 \rangle \langle \Psi_0 | \hat{\beta} | \Psi_I \rangle$ the above equation will reduce to

$$\alpha_{\beta\gamma}(\omega) = \sum_I \frac{2 \langle \Psi_I | \hat{\beta} | \Psi_0 \rangle \langle \Psi_0 | \hat{\gamma} | \Psi_I \rangle}{(E_I - E_0)^2 - \omega^2} \quad (3.7)$$

This expression is interesting due to the fact that it shows the spectroscopic oscillator strengths,

$$f_I = \frac{2}{3} \sum_I (E_I - E_0) \left[|\langle \Psi_0 | \hat{\gamma} | \Psi_I \rangle|^2 + |\langle \Psi_0 | \hat{\beta} | \Psi_I \rangle|^2 \right] \quad (3.8)$$

and the excitation energies $\omega_I = E_I - E_0$ are poles and residues of the mean polarizability,

$$\bar{\alpha}(\omega) = \frac{1}{3} \text{tr}(\alpha(\omega)) = \sum_I \frac{f_I}{\omega_I^2 - \omega^2}. \quad (3.9)$$

For real perturbation, the polarizability will only involve the real part of $\delta P(\omega)$, using Eq.(3.4), the real part of the dynamic polarizability tensor is given by

$$\alpha_{\beta\gamma}(\omega) = -2 \sum_{ij\gamma}^{n_{i\sigma} - n_{j\sigma} > 0} \frac{\beta_{ij\sigma} \Re \delta P_{ij\sigma}}{\epsilon_\gamma}. \quad (3.10)$$

Considering Eq.(2.32), let

$$\mathbf{S}(\omega) = -\mathbf{C}(\mathbf{A} - \mathbf{B})^{-1}\mathbf{C}, \quad (3.11)$$

and

$$\mathbf{\Omega}(\omega) = -\mathbf{S}^{-\frac{1}{2}}(\mathbf{A} + \mathbf{B})^{-1}\mathbf{S}^{-\frac{1}{2}}. \quad (3.12)$$

Using Eqs. (3.11) and (3.12) the real part of the linear response of the density matrix is given by

$$(\Re \delta P(\omega)) = \mathbf{S}^{-\frac{1}{2}} [\omega^2 \mathbf{1} - \mathbf{\Omega}(\omega)]^{-1} \mathbf{S}^{-\frac{1}{2}} (\Re \delta v_{\text{appl}}(\omega)). \quad (3.13)$$

The simplified matrix forms of \mathbf{S} and $\mathbf{\Omega}$ are given by

$$\mathbf{S}(\omega) = -\frac{\delta_{\sigma,\tau} \delta_{i,k} \delta_{j,\ell}}{(n_{k\tau} - n_{\ell\tau})(\epsilon_{k\tau} - \epsilon_{\ell\tau})}. \quad (3.14)$$

and

$$\mathbf{\Omega}(\omega) = \delta_{\sigma,\tau} \delta_{i,k} \delta_{j,\ell} (\epsilon_{\ell\tau} - \epsilon_{k\tau})^2 + 2\sqrt{(n_{i\sigma} - n_{j\sigma})(\epsilon_{j\sigma} - \epsilon_{i\sigma})} K_{i,j,\sigma,k\ell\tau} \sqrt{(n_{k\tau} - n_{\ell\tau})(\epsilon_{\ell\tau} - \epsilon_{k\tau})}. \quad (3.15)$$

Using Eq.(3.13), Eq.(3.10) can be written as

$$\alpha_{\beta\gamma} = 2\beta^\dagger \mathbf{S}^{-\frac{1}{2}} [\boldsymbol{\Omega}(\omega) - \omega^2 \mathbf{1}]^{-1} \mathbf{S}^{-\frac{1}{2}} \gamma \quad (3.16)$$

The excitation energies and the oscillator strengths are obtained by comparing the above equation with the sum-over-states (SOS) formula for the polarizability. Since $\alpha(\omega)$ has poles at the excitation energies, ω_I , it follows that the excitation energies are the solutions of the psuedo-eigenvalue problem

$$\boldsymbol{\Omega}(\omega) \mathbf{F}_I = \omega_I^2 \mathbf{F}_I. \quad (3.17)$$

It is also clear from the sum-over-states formula that $\alpha(\omega)$ is even function of ω , thus $\boldsymbol{\Omega}(\omega)$ and $K(\omega)$ must also be even functions of ω , and hence Eq.(2.24) are hermitian matrices.

Taking the spectral expansion of the sum-over-states formula, we have

$$[\boldsymbol{\Omega}(\omega) - \omega^2 \mathbf{1}]^{-1} = \sum_I \frac{R_I}{\omega_I^2 - \omega^2} \mathbf{F}_I \mathbf{F}_I^\dagger. \quad (3.18)$$

Note that $R_I \neq 1$ if the pseudo-eigenvectors \mathbf{F}_I^\dagger are normalized to 1 (unless $\boldsymbol{\Omega}$ is independent of ω). Instead, it is convenient to normalize the \mathbf{F}_I^\dagger such that $R_I = 1$.

The value of R_I is most easily determined for non-degenerate states, in which case

$$[\boldsymbol{\Omega}(\omega) - \omega^2 \mathbf{1}]^{-1} \cong \frac{R_I}{\omega_I^2 - \omega^2} \mathbf{F}_I \mathbf{F}_I^\dagger, \quad (3.19)$$

near $\omega = \omega_I$. Then

$$R_I^{-1} \cong \mathbf{F}_I^\dagger \frac{\boldsymbol{\Omega}(\omega) - \omega^2 \mathbf{1}}{\omega^2 - \omega_I^2} \mathbf{F}_I \longrightarrow \mathbf{F}_I^\dagger \left[1 - \left[\frac{\partial \boldsymbol{\Omega}(\omega)}{\partial \omega^2} \right]_{\omega=\omega_I} \right] \mathbf{F}_I, \quad (3.20)$$

as $\omega \longrightarrow \omega_I$. Renormalizing the pseudo-eigenvectors such that

$$\mathbf{F}_I^\dagger \left[1 - \left[\frac{\partial \boldsymbol{\Omega}(\omega)}{\partial \omega^2} \right]_{\omega=\omega_I} \right] \mathbf{F}_I = 1, \quad (3.21)$$

then yields $R_I = 1$. Hence \mathbf{F}_I will always refer to these normalized pseudo-eigenvectors. Rewriting the expression for the dynamic polarizability using the spectral expansion in terms of the renormalized \mathbf{F}_I , and comparing with the sum-over-states formula Eq.(3.7) we get

$$\beta^\dagger \mathbf{S}^{-\frac{1}{2}} \mathbf{F}_I = \omega_I^{\frac{1}{2}} \langle \Psi_0 | \hat{\gamma} | \Psi_I \rangle \quad (3.22)$$

so that the oscillator strength is given by

$$f_I = \frac{2}{3} \left[|\mathbf{x}^\dagger \mathbf{S}^{-\frac{1}{2}} \mathbf{F}_I|^2 + |\mathbf{y}^\dagger \mathbf{S}^{-\frac{1}{2}} \mathbf{F}_I|^2 + |\mathbf{z}^\dagger \mathbf{S}^{-\frac{1}{2}} \mathbf{F}_I|^2 \right]. \quad (3.23)$$

This expression derived by us is very useful for optical properties of semiconductor nanostructures.

3.2 Approximation of the Exchange-Correlation Kernel

For simplicity we can split the exchange-correlation kernel given in Eq. (2.21) in to two parts: $K = K^{(I)} + K^{(II)}$. The first term represents a double integral over $\frac{1}{|\mathbf{r}-\mathbf{r}'|}$. Instead of performing the costly double integration by direct summation, we calculate this term by solving the Poisson equation with in the boundary domain. The Conjugate gradient method is employed to solve this equation.

$$\nabla^2 \Phi_{ij\sigma} = -4\pi \psi_{i\sigma}(\mathbf{r}) \psi_{j\sigma}(\mathbf{r}). \quad (3.24)$$

The first term in Eq.(2.21) is calculated as

$$K_{ij\sigma, k\ell\tau}^{(I)} = \int \Phi_{ij\sigma}(\mathbf{r}) \psi_{k\tau}(\mathbf{r}) \psi_{\ell\tau}(\mathbf{r}) d\mathbf{r}. \quad (3.25)$$

The second term in Eq. (2.21) represents a double integral over the functional derivative of the exchange-correlation energy, $\delta^2 E_{xc}[\rho]/\delta\rho_\sigma(\mathbf{r})\delta\rho_\tau(\mathbf{r}')$. Within the local approximation of the exchange-correlation potential this term is reduced to a single integral,

$$K_{ij\sigma, k\ell\tau}^{(II)} = \int \psi_{i\sigma}(\mathbf{r})\psi_{j\sigma}(\mathbf{r}) \frac{\delta^2 E_{xc}[\rho]}{\delta\rho_\sigma(\mathbf{r})\delta\rho_\tau(\mathbf{r})} \psi_{k\tau}(\mathbf{r})\psi_{\ell\tau}(\mathbf{r}) d\mathbf{r}. \quad (3.26)$$

The above equation requires the evaluation of the second derivatives for the spin-up and spin-down charge densities. The LDA exchange energy per particle is normally approximated by that of the homogeneous electron gas [7],

$$\epsilon_x[\rho_\sigma(\mathbf{r})] = -\frac{3}{4\pi} (6\pi^2\rho_\sigma(\mathbf{r}))^{\frac{1}{3}} \quad \sigma = \{\uparrow, \downarrow\}. \quad (3.27)$$

The first derivative of the total exchange energy determines the LDA exchange potential,

$$\frac{\delta E_x[\rho]}{\delta\rho_\sigma} = v_x[\rho_\sigma] = -\frac{1}{\pi} (6\pi^2\rho_\sigma(\mathbf{r}))^{\frac{1}{3}} \quad \sigma = \{\uparrow, \downarrow\}. \quad (3.28)$$

The second derivatives are:

$$\frac{\delta^2 E_x[\rho]}{\delta\rho_\uparrow\delta\rho_\uparrow} = -\left(\frac{2}{9\pi}\right)^{\frac{1}{3}} \rho_\downarrow^{-\frac{2}{3}}, \quad \frac{\delta^2 E_x[\rho]}{\delta\rho_\uparrow\delta\rho_\downarrow} = 0. \quad (3.29)$$

A parameterized form of Ceperley-Alder functional [8] can be used for the LDA correlation energy. This functional is based on two different analytical expressions for $r_s < 1$ and $r_s \geq 1$, where $r_s = (3/4\pi\rho)^{1/3}$ is the local Seitz radius and $\rho = \rho_\uparrow + \rho_\downarrow$. One can adjust the parameter for $r_s < 1$ to guarantee a continuous second derivative of the correlation energy. The adjusted interpolation formula for the correlation energy per particle is given by

$$\epsilon_c^{U,P} = \begin{cases} A \ln r_s + B + Cr_s \ln r_s + Dr_s + Xr_s^2 \ln r_s & r_s < 1 \\ \gamma/(1 + \beta_1\sqrt{r_s} + \beta_2r_s) & r_s \geq 1, \end{cases} \quad (3.30)$$

Spin	A	B	C	D	X	γ	β_1	β_2
Unpolarized	0.0311	-0.048	-0.0015	0.0116	0.0036	-0.1423	1.0529	0.3334
Polarized	0.01555	-0.0269	-0.0005	-0.0048	0.0012	-0.0843	1.3981	0.2611

Table 3.1: Fitting parameters in the interpolation formula for the correlation energy given by Eq.(3.30). The data is taken from Ref. [8].

where two separate sets of coefficients are used for the polarized spin (P) and unpolarized spin (U) cases. The numerical values of all fitting parameters appearing in Eq. (3.30) are listed in Table (3.1). Based on this interpolation formula, the first and second derivatives of the total correlation energy can be calculated.

Equations (3.27) - (3.30) describe only the cases of the completely polarized and unpolarized spin. For intermediate spin polarizations, the correlation energy can be obtained with a simple interpolation formula,

$$\epsilon_c = \epsilon_c^U + \xi(\rho)[\epsilon_c^P - \epsilon_c^U], \quad (3.31)$$

where

$$\xi(\rho) = \frac{1}{1 - 2^{-1/3}} \left(x_\uparrow^{4/3} + x_\downarrow^{4/3} - 2^{-1/3} \right); \quad \text{with} \quad x_\uparrow = \frac{\rho_\uparrow}{\rho}, \quad x_\downarrow = \frac{\rho_\downarrow}{\rho}. \quad (3.32)$$

The expression for the second derivative of the correlation energy in case of an arbitrary spin polarization can be written as

$$\begin{aligned} \frac{\delta^2 E_c[\rho]}{\delta \rho_\sigma \delta \rho_\tau} &= \frac{\delta^2 E_c^U}{\delta \rho^2} + \xi(\rho) \left(\frac{\delta^2 E_c^P}{\delta \rho^2} - \frac{\delta^2 E_c^U}{\delta \rho^2} \right) \\ &+ \left(\frac{\partial \xi(\rho)}{\partial \rho_\sigma} + \frac{\partial \xi(\rho)}{\partial \rho_\tau} \right) \left(\frac{\delta E_c^P}{\delta \rho} - \frac{\delta E_c^U}{\delta \rho} \right) \\ &+ \frac{\partial^2 \xi(\rho)}{\partial \rho_\sigma \partial \rho_\tau} \rho (\epsilon_c^P - \epsilon_c^U), \quad \sigma, \tau = \{\uparrow, \downarrow\}, \end{aligned} \quad (3.33)$$

where the spin polarization function, $\xi(\rho)$, and its derivatives are given by

$$\frac{\partial \xi(\rho)}{\partial \rho_\uparrow} = \frac{4}{3\rho(1 - 2^{-1/3})} \left(x_\uparrow^{1/3} - x_\uparrow^{4/3} - x_\downarrow^{4/3} \right), \quad (3.34)$$

$$\frac{\partial^2 \xi(\rho)}{\partial \rho_\uparrow \partial \rho_\uparrow} = \frac{4}{9\rho^2 (1 - 2^{-1/3})} \left(x_\uparrow^{-2/3} - 8x_\uparrow^{1/3} + 7(x_\uparrow^{4/3} + x_\downarrow^{4/3}) \right), \quad (3.35)$$

$$\frac{\partial^2 \xi(\rho)}{\partial \rho_\uparrow \partial \rho_\downarrow} = \frac{4}{9\rho^2 (1 - 2^{-1/3})} \left(7(x_\uparrow^{4/3} + x_\downarrow^{4/3}) - 4(x_\uparrow^{1/3} + x_\downarrow^{1/3}) \right). \quad (3.36)$$

The TDLDA formalism presented in previous sections can be further simplified for systems with the unpolarized spin. In this case, the spin-up and spin-down charge densities are equal, $\rho_\uparrow = \rho_\downarrow$, and Eqs. (3.32), (3.34)-(3.36) yield

$$\xi(\rho) = 0, \quad \frac{\partial^2 \xi(\rho)}{\partial \rho_\uparrow \partial \rho_\uparrow} = \frac{4}{9\rho^2 (2^{1/3} - 1)} \quad (3.37)$$

$$\frac{\partial \xi(\rho)}{\partial \rho_\uparrow} = 0, \quad \frac{\partial^2 \xi(\rho)}{\partial \rho_\uparrow \partial \rho_\downarrow} = -\frac{4}{9\rho^2 (2^{1/3} - 1)} \quad (3.38)$$

Since the coordinate parts of spin-up and spin-down Kohn-Sham wavefunctions for systems with the unpolarized spin are identical, $\psi_{i\uparrow} = \psi_{i\downarrow}$, it follows that $\Omega_{ij\uparrow, k\ell\uparrow} = \Omega_{ij\downarrow, k\ell\downarrow}$ and $\Omega_{ij\uparrow, k\ell\downarrow} = \Omega_{ij\downarrow, k\ell\uparrow}$. This allows us to separate "singlet" and "triplet" transitions by representing Eq. (3.17) in the basis set of $\{\mathbf{F}_+, \mathbf{F}_-\}$, chosen as

$$\mathbf{F}_{ij}^{\{+, -\}} = \frac{1}{\sqrt{2}} (\mathbf{F}_{ij\uparrow} \pm \mathbf{F}_{ij\downarrow}). \quad (3.39)$$

In this basis, the matrix $\mathbf{\Omega}$ becomes

$$\mathbf{\Omega}_{ij, k\ell}^{\{+, -\}} = \delta_{i,k} \delta_{j,\ell} \omega_{k,\ell}^2 + 2\sqrt{(n_{i\sigma} - n_{j\sigma})(\epsilon_{j\sigma} - \epsilon_{i\sigma})} \mathbf{K}_{ij, k\ell}^{\{+, -\}} \sqrt{(n_{k\tau} - n_{\ell\tau})(\epsilon_{\ell\tau} - \epsilon_{k\tau})}, \quad (3.40)$$

where $\mathbf{K}_{ij, k\ell}^{\{+, -\}} = \mathbf{K}_{ij\uparrow, k\ell\downarrow}$. The components of $\mathbf{K}^{\{+, -\}}$ in their explicit form are given by

$$\begin{aligned} \mathbf{K}_{ij, k\ell}^+ &= 2 \int \int \frac{\psi_i(\mathbf{r}) \psi_j(\mathbf{r}') \psi_\ell(\mathbf{r}')}{|\mathbf{r} - \mathbf{r}'|} d\mathbf{r} d\mathbf{r}' \\ &+ 2 \int \psi_i(\mathbf{r}) \psi_j(\mathbf{r}) \left(\frac{\delta^2 E_c^U}{\delta \rho^2} - \frac{1}{(9\pi)^{1/3} \rho^{2/3}} \right) \psi_k(\mathbf{r}) \psi_\ell(\mathbf{r}) d\mathbf{r}, \end{aligned} \quad (3.41)$$

$$\mathbf{K}_{ij,k\ell}^- = 2 \int \psi_i(\mathbf{r})\psi_j(\mathbf{r}) \left(\frac{4(\epsilon_c^P - \epsilon_c^U)}{9(2^{1/3} - 1)} - \frac{1}{(9\pi)^{1/3}\rho^{2/3}} \right) \psi_k(\mathbf{r})\psi_\ell(\mathbf{r})d\mathbf{r}. \quad (3.42)$$

For most practical applications, only "singlet" transitions represented by the \mathbf{F}_+ basis vectors are of interest. Triplet transitions described by the \mathbf{F}_- vectors have zero dipole oscillator strength and do not contribute to optical absorption. This analytical result is new to the best of our knowledge and can be refined computationally to make contact with experimental observation on silicon nanostructures.

3.3 Calculation of Optical Gap

The first step in the calculation of optical gap involves the calculation of the quasi-particle gap, which is the energy needed to create a non-interacting electron-hole pair. The second component is due to the direct Coulomb (E_{Coul}) and exchange (E_{ex}) electron-hole interactions comprising the exciton binding energy. These parameters determine the optical properties of silicon nanostructures, is called HOMO-LUMO gap.

For an n-electron system, the quasi-particle gap ε_g^{qp} can be expressed in terms of the ground state total energies E of the (n+1)-, (n-1)-, and n-electron system as

$$\varepsilon_g^{qp} = (E_{n+1} - E_n) - (E_n - E_{n-1}) = E_{n+1} + E_{n-1} - 2E_n = \varepsilon_g^{HL} + \Sigma, \quad (3.43)$$

where Σ is the self-energy correction to the HOMO-LUMO gap ε_g^{HL} obtained with in LDA. This definition is quite convenient for the calculation of the quasi-particle gap, as it is possible to excite individual electrons or holes from the ground state to electronic configuration of a confined system. Eq. (3.43) yields the correct quasi-particle gap ε_g^{qp} if the exchange-correlation functional is used.

Quantum confinement in nanostructures enhances the bare exciton Coulomb interaction, and reduces the electronic screening so that the exciton Coulomb energy becomes comparable to the quasi-particle gap,

$$\varepsilon_g^{opt} = \varepsilon_g^{qp} - E_{Coul}, \quad (3.44)$$

Since the exciton exchange-correlation energies are much smaller than E_{Coul} for the quantum dots it will be neglected. E_{Coul} is better calculated using ab initio pseudo-wavefunctions. The exciton Coulomb energy can be written as

$$\begin{aligned} E_{Coul} &= \int d\mathbf{r}_1 |\psi_e(\mathbf{r}_1)|^2 V_{scr}^h(\mathbf{r}_1), \\ &= \int d\mathbf{r}_1 |\psi_e|^2 \int d\mathbf{r} \epsilon^{-1}(\mathbf{r}_1, \mathbf{r}_2) V_{unscr}^h(\mathbf{r}), \\ &= \int \int \int \epsilon^{-1}(\mathbf{r}_1, \mathbf{r}_2) \frac{|\psi_e(\mathbf{r}_1)|^2 |\psi_h(\mathbf{r}_2)|^2}{|\mathbf{r} - \mathbf{r}_2|} d\mathbf{r} d\mathbf{r}_1 d\mathbf{r}_2. \end{aligned} \quad (3.45)$$

In the above expression V_{scr}^h and V_{unscr}^h are the screened and unscreened potentials due to holes, ψ_e and ψ_h are the electron and hole wavefunctions respectively, and $\epsilon^{-1}(\mathbf{r}_1, \mathbf{r}_2)$ is the inverse of the microscopic dielectric matrix. One can define $\epsilon^{-1}(\mathbf{r}_1, \mathbf{r}_2)$ as

$$\int \frac{\epsilon^{-1}(\mathbf{r}_1, \mathbf{r}_2)}{|\mathbf{r} - \mathbf{r}_1|} d\mathbf{r} \equiv \frac{\tilde{\epsilon}^{-1}(\mathbf{r}_1, \mathbf{r}_2)}{|\mathbf{r}_1 - \mathbf{r}_2|}. \quad (3.46)$$

Then the exciton Coulomb energy can be written as

$$E_{Coul} = \int \int \tilde{\epsilon}^{-1}(\mathbf{r}_1, \mathbf{r}_2) \frac{|\psi_e(\mathbf{r}_1)|^2 |\psi_h(\mathbf{r}_2)|^2}{|\mathbf{r}_1 - \mathbf{r}_2|} d\mathbf{r}_1 d\mathbf{r}_2, \quad (3.47)$$

if $\tilde{\epsilon}^{-1}(\mathbf{r}_1, \mathbf{r}_2)$ is taken to be unity the unscreened Coulomb energy can be determined.

In order to calculate Eq.(3.47), $\epsilon(\mathbf{r}_1, \mathbf{r}_2)$ needs to be calculated. Within density functional linear response theory, $\epsilon(\mathbf{r}_1, \mathbf{r}_2)$ can be shown to have

$$\epsilon(\mathbf{r}_1, \mathbf{r}_2) = \delta(\mathbf{r}_1, \mathbf{r}_2) - \int d\mathbf{r} \left[\frac{1}{|\mathbf{r}_1 - \mathbf{r}|} + \frac{\delta^2 E_{xc}}{\delta\rho(\mathbf{r}_1)\delta\rho(\mathbf{r})} \right] \chi_0(\mathbf{r}, \mathbf{r}_2), \quad (3.48)$$

where E_{xc} is the exchange correlation functional and $\chi_0(\mathbf{r}, \mathbf{r}_2)$ is the independent particle polarizability:

$$\chi_0(\mathbf{r}, \mathbf{r}_2) = \sum_{i,j} (n_i - n_j) \frac{\psi_i^*(\mathbf{r})\psi_j(\mathbf{r})\psi_j^*(\mathbf{r}_2)\psi_i(\mathbf{r}_2)}{\epsilon_i - \epsilon_j}, \quad (3.49)$$

as expressed in terms of the Kohn-Sham wavefunctions and eigenvalues, $\psi_i(\mathbf{r})$ and ϵ_i having occupation number n_i .

With real wavefunctions and integer occupation numbers, the expression for ϵ can be simplified by taking spin degeneracy into account as,

$$\epsilon(\mathbf{r}_1, \mathbf{r}_2) = \delta(\mathbf{r}_1, \mathbf{r}_2) + 4 \sum_{v,c} [J_{vc}(\mathbf{r}_1) + K_{vc}(\mathbf{r}_1)] \frac{\psi_v(\mathbf{r}_2)\psi_c(\mathbf{r}_2)}{\epsilon_c - \epsilon_v}, \quad (3.50)$$

where the summations v and c , are over the valence and conduction orbitals, and the integrals $J_{vc}(\mathbf{r})$ and $K_{vc}(\mathbf{r})$ are defined as

$$J_{vc}(\mathbf{r}_1) = \int d\mathbf{r} \frac{\psi_v\psi_c}{|\mathbf{r}_1 - \mathbf{r}|} \quad (3.51)$$

and

$$K_{vc}(\mathbf{r}_1) = \int d\mathbf{r} \frac{\delta^2 E_{xc}}{\delta\rho(\mathbf{r}_1)\delta\rho(\mathbf{r})} \psi_v\psi_c = \frac{\delta^2 E_{xc}}{\delta\rho^2(\mathbf{r}_1)} \psi_v\psi_c. \quad (3.52)$$

For calculating exciton Coulomb energies, the inverse of the $\epsilon(\mathbf{r}, \mathbf{r}')$ matrix is needed. We can express the matrix ϵ in terms of identity matrix I and rank $N_{vc} = N_v \times N_c$ matrices U and V , where N_v and N_c are the number of valence and conduction orbitals, respectively. The matrices U and V are defined as $U = 2(J_{vc} + K_{vc})$ and $V = \frac{2\psi_v\psi_c}{\epsilon_c - \epsilon_v}$ for which the rows are labelled (from 1 to N) by grid points, and the columns are labelled (from 1 to N_{vc}) by valence and conduction orbital pairs. This leads to the following matrix expression for the response function:

$$\epsilon = I + UV^T, \quad (3.53)$$

where V^T is the transpose of matrix V . Expressing the ϵ matrix in this fashion allows us to calculate its inverse in terms of the inverse of the matrix $X = I + V^T U$ as follows:

$$\epsilon^{-1} = (I + UV^\dagger)^{-1} = I - U\chi^{-1}V^T. \quad (3.54)$$

On a Cartesian grid of uniform spacing h , the elements of the inverse dielectric matrix can finally be written as

$$\epsilon_{ij} = \frac{1}{h^3} \left(\delta_{ij} - \sum_{k\ell=i}^{N_{vc}} U_{i,k} X_{k\ell}^{-1} V_{\ell,j}^T \right). \quad (3.55)$$

We note that X is a $N_{vc} \times N_{vc}$ matrix.

3.4 Computational Methods

Our computational technique is based on the higher-order finite difference pseudopotential method [9]. We use the local density approximation of Ceperely and Alder [8]. The solution proceeds in three parts: First, the Kohn-Sham energies and wave functions are found by means of a conventional ground state calculation. Second, the wavefunctions are used to construct the coupling matrix, Eq. (2.21). Third, the TDLDA eigenvalue equation, Eq. (3.17) is solved and the absorption spectrum is constructed. All these steps are performed using-real space grid confined in a spherical domain.

A key aspect of our work is the availability of higher order expansions for the kinetic-energy operator, that is, expansion of the Laplacian. We impose a simple,

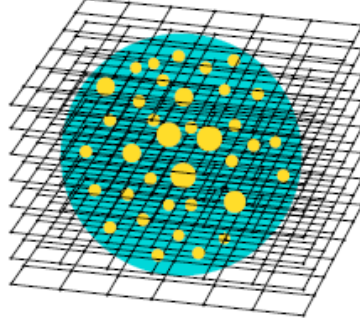


Figure 3.1: Uniform grid illustrating a typical configuration for examining the electronic structure of a localized system. The gray sphere represents the domain where the wavefunctions are allowed to be non-zero. The light spheres within the domain are atoms.

uniform orthogonal three dimensional grid on our system where the points are described in a finite domain by (x_i, y_j, z_k) . We approximate $\frac{\partial^2 \psi}{\partial x^2}$ at (x_i, y_j, z_k) by

$$\frac{\partial^2 \psi}{\partial x^2} = \sum_{n=-N}^{n=N} C_n \psi(x_i + nh, y_i, z_k) + O(h^{2N+2}), \quad (3.56)$$

where h is the grid spacing and N is a positive integer. This approximation is accurate to $O(h^{2N+2})$ upon the assumption that ψ can be approximated accurately by a power series in h . Algorithms are available to compute the coefficients C_n for arbitrary order in h . Expansion coefficients for a uniform grid are shown in Table 3.2.

-	C_i	C_{i+1}	C_{i+2}	C_{i+3}	C_{i+4}	C_{i+5}	C_{i+6}
N=1	-2	1	0	0	0	0	0
N=2	$-\frac{5}{2}$	$\frac{4}{3}$	$-\frac{1}{12}$	0	0	0	0
N=3	$-\frac{49}{18}$	$\frac{2}{3}$	$-\frac{1}{12}$	$\frac{1}{90}$	0	0	0
N=4	$-\frac{205}{72}$	$\frac{8}{5}$	$-\frac{1}{5}$	$\frac{8}{315}$	$-\frac{1}{560}$	0	0
N=5	$-\frac{5269}{1800}$	$-\frac{5}{3}$	$-\frac{2}{21}$	$-\frac{5}{126}$	$-\frac{5}{1008}$	$\frac{1}{3150}$	0
N=6	$-\frac{5369}{1800}$	$\frac{12}{7}$	$-\frac{15}{56}$	$\frac{10}{119}$	$-\frac{1}{112}$	$\frac{2}{1925}$	$-\frac{1}{16632}$

Table 3.2: Expansion coefficients $C_n, n = 0, \dots, \pm N$, for higher-order finite-difference expressions of the second derivative [12].

Within the kinetic energy operator expanded as in Eq.(3.56), one can set up a

one electron *Schrödinger* equation over the grid. We will employ the local-density approximation in setting up the *Schrödinger* equation. We solve for $\psi(x_i, y_j, z_k)$ on the grid by the secular equation:

$$\begin{aligned}
& - \frac{\hbar^2}{2m} \left\{ \sum_{n_1=-N}^{n_1=N} C_{n_1} \psi(x_i + n_1 h, y_j, z_k) + \sum_{n_2=-N}^{n_2=N} C_{n_2} \psi(x_i, y_j + n_2 h, z_k) \right. \\
& + \left. \sum_{n_3=-N}^{n_3=N} C_{n_3} \psi(x_i, y_j, z_k + n_3 h) \right\} + \left[V_{ion}(x_i, y_j, z_k) \right. \\
& + \left. V_H(x_i, y_j, z_k) + V_{xc}(x_i, y_j, z_k) \right] \psi(x_i, y_j, z_k) \\
& = E(x_i, y_j, z_k) \psi(x_i, y_j, z_k)
\end{aligned} \tag{3.57}$$

If there are M grid points, the size of the full matrix resulting the above eigenvalue problem is $M \times M$. V_{ion} is the nonlocal ionic pseudopotential, V_H is the Hartree potential, and V_{xc} is the local-density expression for the exchange correlation potential. The two parameters used in setting up the matrix are the grid spacing h , and the order N .

Chapter 4

Result and Discussion

To assess the accuracy of the TDLDA formalism, we computed excitation energies for four hydrogenated silicon molecules. Calculations were performed inside a spherical boundary domain with a radius of 15 a.u. For all atoms, we included 25 unoccupied states, which described transitions to both bound and continuum levels. We observed no noticeable change in the computed excitation energies and oscillator strengths upon further increase of the boundary domain or the number of unoccupied states included in the calculations.

Absorption Spectra of Si_nH_m clusters were calculated in two steps. First, the minimum energy cluster structure were obtained using real space pseudopotential method and LDA exchange-correlation potential. The optimized geometries of Si_nH_m clusters are shown in Fig.(4.1). Before proceeding with TDLDA calculations, we carefully tested the computed excitation energies and absorption spectra for convergence. For all clusters we require at least 10-20 a.u. separation between surface atoms and the computational domain. The calculation of TDLDA included at least two to three

times as many unoccupied states. These conditions were sufficient to achieve convergence of the computed spectra in the experimentally important region below 10 eV.

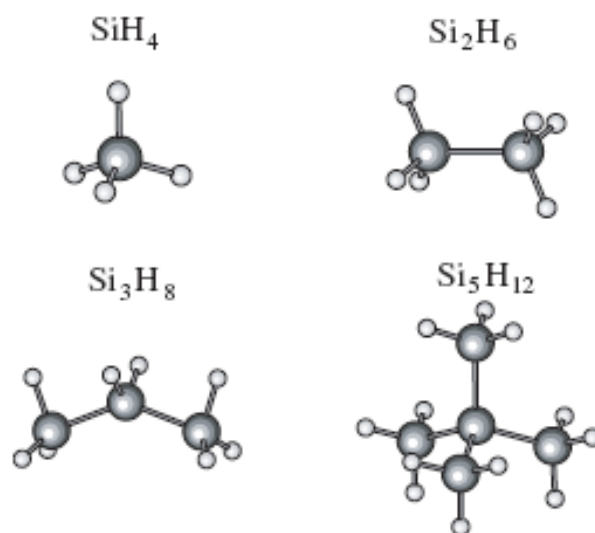


Figure 4.1: Optimized Structure of Si_nH_m clusters.

In table (4.1), we compare TDLDA values for the excitation energies of the four Si_nH_m clusters with experimental data [10]. The table also shows the Kohn-Sham LDA ionization energies of the clusters, $-\epsilon_{HOMO}^{LDA}$, given the negative values of the energies for the highest occupied LDA electronic orbitals.

Cluster	Excitation Energies		Ionization Energy
	Experiment	TDLDA	$-\epsilon_{HOMO}^{LDA}$
SiH_4	8.8	8.3	8.6
	9.7	9.2	
	10.7	9.7	
Si_2H_6	7.6	7.2	7.5
	8.4	8.610	
Si_3H_8	6.6	6.2	6.9
	7.5	7.0	
	9.3	8.8	
Si_5H_{12}	6.5	6.6	7.3

Table 4.1: Excitation and ionization energies of Si_nH_m clusters. Experimental excitation energies are adapted from Ref. [10]. All values are in eV.

The table demonstrates that the calculated TDLDA excitation energies for the transitions below or close to $-\epsilon_{HOMO}^{LDA}$ agree well with the experimental data. This agreement however, deteriorates for higher excitations, which lie above $-\epsilon_{HOMO}^{LDA}$. As the size of the cluster increases, the energy of the first-allowed excitation moves further down from the LDA ionization energy, and the agreement with experiment improves. For larger Si_nH_m clusters, the first-allowed optical transitions are always located below $-\epsilon_{HOMO}^{LDA}$. On this basis, we believe that TDLDA should provide an accurate description of the photo-absorption gaps and the low energy optical transitions in larger Si_nH_m clusters.

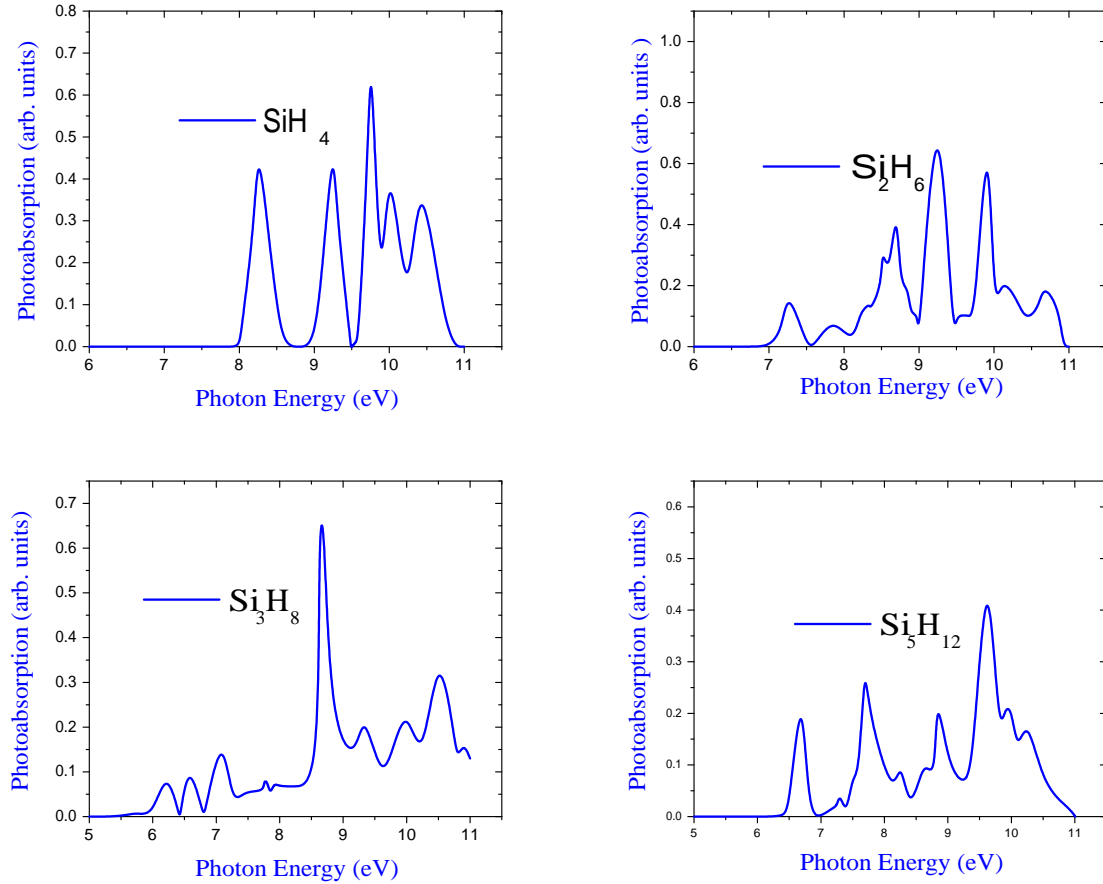


Figure 4.2: Photoabsorption versus photon energy for Si_nH_m clusters.

One of the most fundamental parameters describing the interaction of light with nanocrystals is their absorption cross-section σ . It plays an essential role in modelling of the integral absorption or luminescence properties of nanocrystal assemblies. This value is a product of the density of electronic states and the oscillator strength of the optical transitions. Direct measurement of σ by absorption technique is almost not possible because of the residual size distribution and unknown number of absorbing nanoparticles. Our calculated absorption spectra of Si_nH_m clusters are shown in Figure (4.2). These plots for photo-absorption versus photon energy shows that the

spectra of hydrogenated silicon clusters do not display low energy transitions associated with the surface atoms. This is due to the fact that, surface passivation of silicon quantum dots with hydrogen saturates all dangling bonds as a result the corresponding localized states are removed from the energy range near the Fermi-energy. As depicted in the graph, the lowest optical excitation energy for silane, disilane, trisilane and pentasilane are 8.3, 7.2, 6.2 and 6.6 eV respectively. These data establishes that our first principle calculation agree well with experimental one.

The excitation energy versus cluster size, is shown in Fig. (4.3) using the data obtained through Gaussian 03 package from Chemistry department Addis Ababa University.

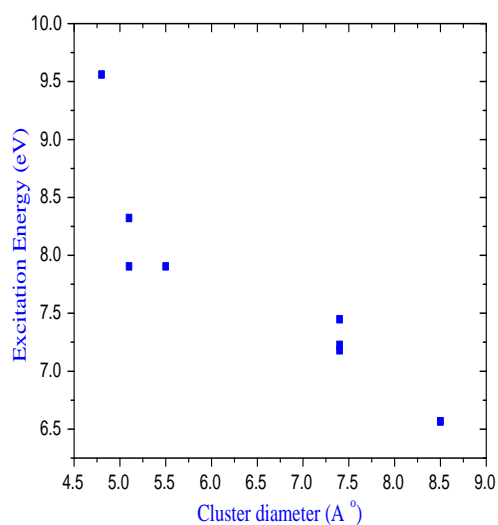


Figure 4.3: Excitation energy versus cluster diameter.

The value of the excitation energy found using the Gaussian 03 software package was also consistent with the experimental and the calculated numerical values. In Fig.(4.3) it is shown that the excitation energy generally decreases with increasing

cluster size.

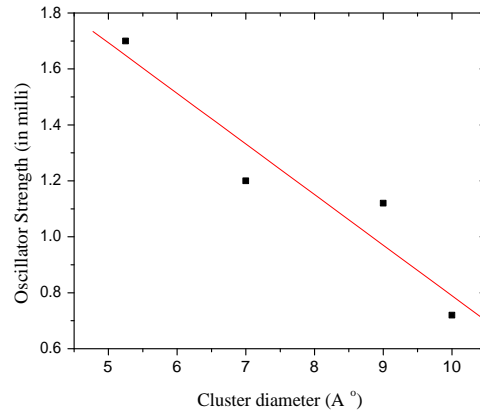


Figure 4.4: Oscillator strength versus Si_nH_m cluster diameter

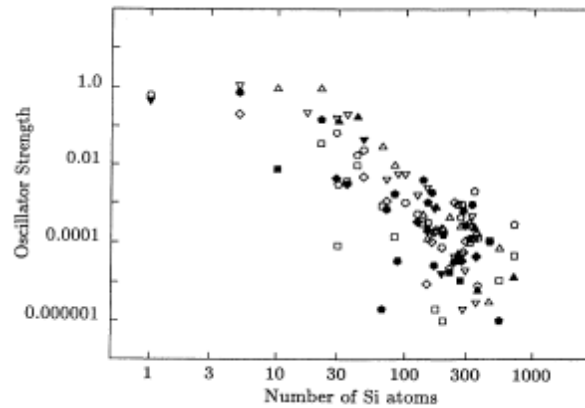


Figure 4.5: Oscillator strength versus number of silicon atom in the cluster.

In small clusters dipole-allowed transitions are possible, which differs from bulk structures, dipole forbidden transitions, due to the confined nature of electronic states. Fig.(4.4) demonstrates that the oscillator strength of dipole-allowed transitions near the absorption edge decreases with increasing cluster size. Fig.(4.5) is taken for comparison from [10]. Their calculation is based on density functional theory, as can be seen from the graph the result is inconformity of our calculation for small

nanoclusters.

The Optical absorption gaps for small clusters can be defined directly by the energy of the first dipole-allowed transition in their absorption spectra. For large clusters, the absorption spectra become essentially quasi-continuous. The variation of the optical absorption gaps as a function of the cluster size is shown in Figure (4.4). For the selected clusters, SiH_4 , Si_2H_6 , Si_3H_8 , Si_5H_{12} , the gaps computed by the TDLDA methods are close to the experimental values [10]. As depicted in the graph the gap for Si_nH_m clusters gradually decrease as the size of the cluster increases and the discrete spectra for small clusters evolve into quasi-continuous spectra for larger silicon nanocrystals.

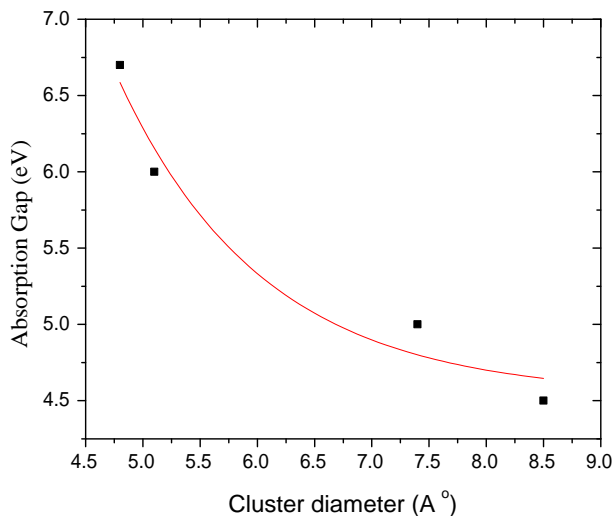


Figure 4.6: Variation of optical absorption gaps as a function of cluster diameter.

This result is in conformity with the recent pseudopotential calculation by Ghoshal et al [11]. Furthermore, they have shown that, the band gap increases as much as 0.13eV on passivation the surface of the dot with hydrogen. So both quantum

confinement and surface passivation determine the optical and electronic properties of Si quantum dots.

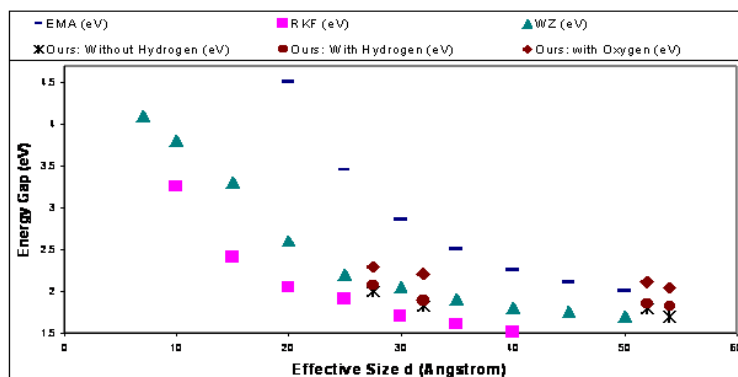


Figure 4.7: LUMO-HOMO band gap versus the effective sizes from Wang and Zunger (triangles), multi band effective mass result (stars), the result of the method of Rama Krishna and Friesner (square boxes) and our result without hydrogen (plus) and with hydrogen (solid circles) [11].

Chapter 5

Conclusion

We have implemented linear-response theory within the time-dependent density functional formalism and the local density approximation (TDLDA) to compute excitation energies and optical absorption spectra of Si_nH_m clusters. The calculated TDLDA excitation energies and absorption spectra for hydrogen-terminated silicon dots were found to be in good agreement with the experiment. The comparison of the spectra calculated with the exact and approximate TDLDA expressions indicates an important role of collective electronic effects.

We have shown that the TDLDA formalism can provide an efficient alternative to more complex theoretical methods for the excited state properties. Compared to other first principles techniques for excited states, TDLDA method requires considerably less computational effort and can be used for much larger systems. At the same time, as a fully ab initio technique, TDLDA avoids many of the controversies associated with empirical and semi-empirical methods.

We have also performed the calculation for excitation energies using Gaussian 03 software package. The first thing to be done here was that the structures of

the quantum dots are optimized after that the excitation energy was computed using time-dependent local density approximation. The results obtained were in conformity with experimental and numerical values.

Bibliography

- [1] P. Hohenberg and W. Kohn, Phys. Rev. **136**, B864 (1964)
- [2] E. Runge and E. K. U. Gross, Phys. Rev. Lett **52** (1984), 997.
- [3] W. Kohn and L. J. Sham, Phys. Rev. **140**, A1133 (1965)
- [4] D. R. Hamann, M. Schluter, and C. Chiang, Phys. Rev. Lett. **43**, 1494 (1979)
- [5] L. Kleinman and D. M. Bylander, Phys. Rev. Lett. **48**, 1425 (1982).
- [6] G. P. Kerker, J. Phys. C **13**, L189 (1980).
- [7] G. D. Mahan, Many-Particle Physics, Plenum Press, New York, 1981.
- [8] D. M. Ceperley and B. Alder, Phys. Rev. Lett. **45**, 566 (1980).
- [9] I. Vasiliev, S.Ougut, and J. R. Chelikowsky, Phys. Rev. B **65**, 115416 (2002).
- [10] B. Delley and E. F. Steigmeier, Phys. Rev. B **47**, 1397 (1993).
- [11] S. K. Ghoshal, Umesh Gupta and Karan Singh, Indian Journal of Pure and Applied Physics, Vol. 43, p.p. 188, March (2005).
- [12] James R. Chelikowsky, N. Troullier, K. Wu, and Y. Saad, Phys. Rev B **50**, (1994)